Article:
Verl, A., Valente, A., Melkote, S. et al. (3 more authors) (2019) Robots in machining. CIRP Annals. ISSN 0007-8506

https://doi.org/10.1016/j.cirp.2019.05.009

CIRP 2028 1–24

ARTICLE IN PRESS

CIRP Annals - Manufacturing Technology xxx (2019) xxx–xxx

Contents lists available at ScienceDirect

CIRP Annals - Manufacturing Technology

journal homepage: http://ees.elsevier.com/cirp/default.asp

Robots in machining

Alexander Verl (2)[a,*], Anna Valente (2)[b], Shreyes Melkote (1)[c], Christian Brecher (1)[d], Erdem Ozturk (2)[e], Lutfi Taner Tunc[f]

[a] Institute for Control Engineering of Machine Tools and Manufacturing Units (ISW), University of Stuttgart, Germany
[b] SUPSI —– University of Applied Sciences and Arts of Southern Switzerland, Switzerland
[c] George W. Woodruff School of Mechanical Engineering, Georgia Institute of Technology, USA
[d] Laboratory for Machine Tools and Production Engineering (WZL), RWTH Aachen University, Germany
[e] Advanced Manufacturing Research Centre (AMRC), The University of Sheffield, UK
[f] Integrated Manufacturing Technologies Research and Application Centre, Faculty of Engineering and Natural Sciences, Sabanci University, Turkey

ARTICLE INFO

Keyword:
Robot
Machining
Process planning
Control

ABSTRACT

Robotic machining centers offer diverse advantages: large operation reach with large reorientation capability, and a low cost, to name a few. Many challenges have slowed down the adoption or sometimes inhibited the use of robots for machining tasks. This paper deals with the current usage and status of robots in machining, as well as the necessary modelling and identification for enabling optimization, process planning and process control. Recent research addressing deburring, milling, incremental forming, polishing or thin wall machining is presented. We discuss various processes in which robots need to deal with significant process forces while fulfilling their machining task.

1. Introduction

Robots are currently used in industrial machining operations which involve relatively low cutting force requirements such as trimming, drilling, and polishing on composite parts, as well as drilling or deburring, grinding, and milling on metal parts. There are several aspects that stimulate the use of robots in machining. The first and main one is the cost — robots cost less compared to machine tools with the same work space.

During the last decade, a new global sales record has been achieved for industrial robots (IRs) almost every year. In 2016, a total of 294,000 units were sold, an increase of 16% compared to the previous year. This number soared to 381,000 units in 2017, another 30% more than the previous year [1]. More than 3 million installed robots are forecasted by 2020, doubling their number in industrial operation since 2014 [2]. According to the International Federation of Robotics (IFR), in 2016, 1.4% of IRs were intended for mechanical cutting, grinding, deburring, milling, and polishing [1]. This number is low compared to non-processing operations like handling or assembly, which demonstrates the lack of the use of robots in machining. However, these developments illustrate the importance of IRs for machining applications.

Within the large set of operating resources, manufacturing robots are computer numerically controlled (CNC) machines conceived for industry for specific material subtraction or deposition functions (e.g., milling, coating, welding or powder blasting), as well as metrology and inspection functions, while flexibly implementing various process strategies by exploiting several end effectors or even hybrid process chains on different metals and non-metallic materials. A manufacturing robot is typically a robotic arm manipulator on a fixed base that performs repetitive tasks within a local work cell [3]. High-speed robots are hazardous and demand the exclusion of humans from robotic work places, where the robots are typically placed inside a cage. In contrast, collaborative robots are considered safe around humans because they operate at low speed and stop moving if they encounter an obstruction.

When it comes to defining machining robots, the attempt to draw a sharp line to differentiate between them and a machine tool is not straightforward in a general sense and depends on the specific scientific and technical discipline (e.g., machine tools are classified as Cartesian robots in the robotics scientific discipline).

The very term “machining” relates to specific technologies implemented with various tools (DIN 8580) but embeds in its etymology the fact that such technologies are implemented on conventional machine tools. Machining robots should be considered a subset of the manufacturing robot family. They can generally be defined as robots executing manufacturing processes, according to DIN 8580.

Like machine tools, machining robots can accomplish multiple machining tasks by exploiting different configurations, kinematic structures and performance targets while integrating a tool (end effector according to the robotics nomenclature) that performs the machining process when in contact with the material. The end effectors integrated on a machining robot can present similar capabilities as tools mounted on machine tools. Their selection

* Corresponding author.
E-mail address: alexander.verl@isw.uni-stuttgart.de (A. Verl).

https://doi.org/10.1016/j.cirp.2019.05.009
0007-8506/© 2019 Published by Elsevier Ltd on behalf of CIRP.

relies upon product and process driven criteria, along with robot payload and dynamics. By means of the tool, machining robots can convert a blank into a final product by executing operations controlled by the robot's controller unit. Similarly to machine tools [4], the motion of a machining robot can be controlled by a CNC unit, as the machining strategy and trajectory are generated by a CAD/CAM (computer aided design/manufacturing) system. The productivity and accuracy of the machining operations depend on the preparation of the numeric control (NC) programs, the robot path planning, motion strategy, and dynamics optimization, together with the robot behavior assessment in the working area.

In metal cutting, for example, there is a growing number of successful installations where robots have been used in a similar manner to a machine tool or to a person carrying a metal cutting hand tool [5]. The current paper will outline and investigate the opportunities and the range of applications where the adoption of robots for machining constitutes an instrumental leverage.

1.1. Standard definition for robots in machining

The first patent for what we would now consider a robot was filed in 1954 by George C. Devol and issued in 1961 [6]. Since then, the conception and exploitation of robots in industry has brought disruptive innovation while posing complex scientific and technical challenges to the scientific communities.

Nowadays, the robot is universally defined as a goal-oriented machine that can sense, plan and act. According to ISO/IEC 2382:2015 (en), a robot is defined as a mechanical device, usually programmable, designed to perform tasks of manipulation or locomotion under automatic control. Similarly, ISO 18646-1:2016 (en) considers a robot as a program actuated mechanism with a degree of autonomy, moving within its environment to perform intended tasks. An industrial robot is, in turn, described as an automatically controlled, reprogrammable, multipurpose manipulator, programmable in three or more axes, which can be either fixed in place or mobile for use in industrial automation applications [7].

In the following sections, we will introduce the theoretical foundations of robotics and then cover the programming tool chain in robotic machining. Then, an overview of several robotic machining processes is presented. Finally, we look at emerging fields of research in this area and draw a number of conclusions.

2. Theoretical foundations

This chapter summarizes the theoretical background needed for robot machining tasks. Using a robot model enables robot programs to predict behavior and process parameters. In order to model a robot, the first section of this chapter describes important mathematical equations and parameter identification methods. Considerations on mechanical and geometrical properties of robots, followed by aspects regarding robot stiffness are then introduced. Furthermore, the static and dynamic behavior of industrial robots is explained, and various test results are presented. Path planning, robot control and process control strategies are also indispensable when preparing robots for new tasks, and are also discussed in detail in this chapter.

2.1. Robot modelling

There are different approaches to describing a mechanical system analytically. The method of Lagrangian equations described in this section is widely used and an easy way to derive equations of motion for rigid body robots.

Let $q \in \mathbb{R}^n$ be coordinates of the joint angles for an industrial robot in the n-dimensional vector space. First, the Lagrangian L is defined as the difference between the total kinetic and the potential energy of the system (T and V, respectively) [8]:

$$L(q, \dot{q}) = T(q, \dot{q}) - V(q) \tag{1}$$

The kinetic and potential energy are described for each link in the system. The potential energy is defined as the product of the mass m_i of the ith link, the gravitational acceleration g, and the height of the center of mass (opposite to the direction of gravity) for the ith link:

$$V_i(q) = m_i g h_i(q) \tag{2}$$

In comparison to the potential energy, the kinetic energy is, however, far more complicated to describe and follows as:

$$T = \frac{1}{2}\dot{q}^T \sum_{i=1}^{n} [m_i J_{v_i}(q)^T J_{v_i}(q) + J_{\omega_i}(q)^T R_i(q) I_i R_i(q)^T J_{\omega_i}(q)]\dot{q} \tag{3}$$

with the rotational transformation R_i and the inertia matrix I_i for each link i. A central part in describing the kinetic energy is the manipulator's Jacobian J which is a $6 \times n$ matrix for a robot with n links. The Jacobian contains parts for the linear velocity J_v and the angular velocity J_ω, which are described exemplary for rotational joints in the following equations [9]:

$$J = \begin{bmatrix} J_v \\ J_\omega \end{bmatrix} \tag{4}$$

with:

$$J_{v_i} = z_{i-1} \times (O_n^0 - O_{i-1}^0) \tag{5}$$

$$J_{\omega_i} = z_{i-1}^0 \tag{6}$$

The Eqs. (5–6) are illustrated in Fig. 1. In this case, z_{i-1}^0 is the rotation of joint i-1 and $(o_n^0 - o_{i-1}^0)$ is the distance between the tool center point (TCP) – marked in Fig. 1 as a point at the tip of the manipulator's nth body – and the joint i – 1. The zero indicates the world frame as reference frame. In the end, the motion equations are described with partial derivatives of the Lagrangian:

$$\frac{d}{dt}\frac{\partial L}{\partial \dot{q}_i} - \frac{\partial L}{\partial q} = \tau_i \tag{7}$$

where τ_i represents the actuator torques and other nonconservative, generalized forces acting on the ith joint. These equations of motion describe the actuator's dynamics without influences such as friction or reaction torques and forces induced by the environment. For more detailed modelling reference is made to the relevant literature [8].

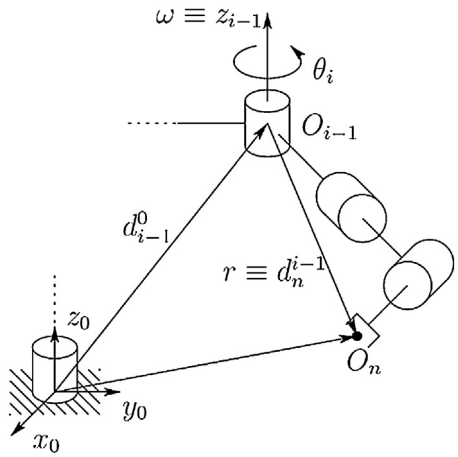

Fig. 1. Calculation of the manipulator's Jacobian [8].

Many system identification approaches have been developed during recent decades in order to determine system parameters like masses, components of the inertia matrix, components of the moments for each link, as well as friction parameters and motor inertias. Most dynamic identification methods for robots use the inverse dynamic identification model, which calculates motor torques with the aforementioned equations of motion. Furthermore, least squares techniques are used to estimate the

Please cite this article in press as: A. Verl, et al., Robots in machining, (2019), https://doi.org/10.1016/j.cirp.2019.05.009

parameters. In some cases, a few parameters like masses or kinematics are already known and therefore do not need to be identified. As the optimal method depends on the robot and on these known parameters, reference is made to literature contributions on these topics [10–12]. In addition, there are many ways to optimize path planning for data acquisition for the identification process. To increase the least squares methods convergence rate and lower the susceptibility to noise, an optimal excitement and implicitly an optimal trajectory is crucial for the process. Hence, a sequential identification process is often used for estimating the different parameters with adapted trajectories [13].

2.2. Methods to describe mechanical and geometrical properties

Machining of a workpiece requires a geometrical description of the machining task and a reference coordinate system in which the task is described. The task described in these coordinate systems is then converted to the machine coordinate system by probing. To execute the machining task, a further transformation to the machine axis coordinate system (or joint coordinate system) is required. Machine tool structures with three translational and optional rotational axes have known and defined transformations. This is not the case for robotic structures including mostly rotational axes with optional translation axes.

In robotics literature, the so-called Denavit–Hartenberg (DH) convention [14] is considered to be the defining set of rules on how to attach these coordinate systems to the robots' linkages. The underlying principle of the DH method is describing the transformation between two linkages with only four parameters, representing a combination of two rotations and two translations [15]. The six parameters generally needed are reduced to four by applying the convention's rules — and limitations. Although the underlying principle remains the same, four different variants of notations are used in scientific literature [16]. Classification is based on the index linkages and parameters, which, in consequence, affects the grouping order of the transformation matrices of the rotations and translations. Instead of attaching only one coordinate system to each joint, the Sheth–Uicker (SU) convention [17] attaches two, an input and an output coordinate system. The relative motion between the two is exactly the joint motion between the two linkages. The DH parameters can still be used to describe the relative transformation between the two coordinate systems attached to one linkage, however, the joint variable term of the DH parameters for the linkage transformation is only a constant offset. Although the DH convention operates with half as many transformations as the SU convention, it is worth noting that the SU convention allows for a more convenient way to define coordinate systems of mechanisms that are not strictly serial. It can also handle complex joint types more conveniently, with more than one degree of freedom.

2.3. Robot stiffness

Robot stiffness is the key parameter that influences machining accuracy. Specifically, the limited static and dynamic stiffness of robot joints and links results in insufficient rigidity of the robot TCP, which in turn impacts the machining accuracy. As pointed out by Pan et al. [18], the static Cartesian stiffness of industrial robots is on the order of 1 N/μm while the corresponding stiffness of a typical CNC machine tool is up to 50 times higher. Unlike a CNC machine tool, the Cartesian stiffness of an industrial robot varies with its joint configuration (or pose) throughout the workspace [19], which complicates the task of machining process control. The magnitude and nature of robot deflections are a function of the magnitude and frequency content of the process forces generated during machining.

In recent years, the effects of machining process parameters and robot configuration on the dynamic characteristics of the robotic machining process and its stability have been investigated. Bondarenko et al. [20] presented a simulation study of the effect of robot dynamics on the instantaneous tool-workpiece interaction in robotic milling with a KUKA KR270 industrial robot. They modelled and analyzed the effect of robot compliance on the instantaneous tool tip displacement due to periodically varying milling forces. However, they did not consider the effect of robot compliance on the milling forces themselves. Recently, Cen and Melkote [21] modelled and analyzed the effect of robot compliance on the instantaneous milling forces. Through simulation and experiments, they showed that the peak milling force (Fig. 2), and hence the tool tip deflection, can be significantly under predicted if this effect is ignored. This effect is important in accounting for offline robot compliance compensation strategies.

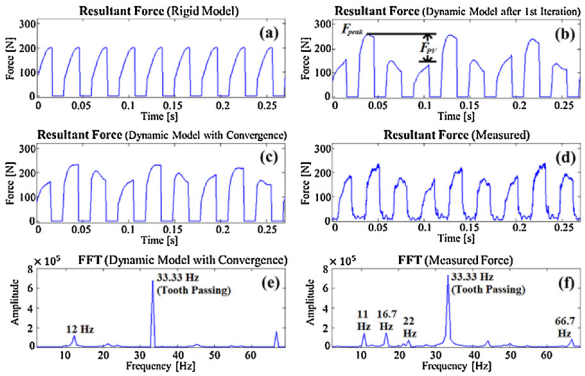

Fig. 2. Effect of robot dynamics on predicted and measured milling forces and their frequency contents [21]. Rigid model (a) ignores robot compliance.

Recently, Cordes et al. [22] presented a detailed analytical study of chatter in robotic milling of aluminum and titanium structures. Their work shows that the robot's pose-dependent vibration modes result in chatter only at low spindle speeds (when milling titanium). In contrast, only pose-independent vibration modes cause chatter at high spindle speeds (when machining aluminum). They subsequently developed a stability chart that can be used to select chatter-free spindle speeds when machining aluminum. In their robotic milling experiments on a KUKA KR210 IR, Cen et al. [23] also found that chatter instability occurs more readily when milling in one Cartesian coordinate direction compared to milling in a direction orthogonal to it. Mousavi et al. [24] have also shown that the natural frequencies of a serial-link robot can vary significantly along a tool path due to a continuously changing robot configuration. They used three dimensional Euler–Bernoulli beam elements with a matrix structural analysis technique. Similar findings have been reported for a parallel kinematic robot (hexapod) [25]. These observations emphasize the importance of accounting for robot dynamics during robot trajectory (motion) plan generation for machining applications.

2.4. Measurement of static properties

Karim et al. [26] analyzed the Cartesian static compliance behavior of a KUKA KR500-3 MT robot in numerous poses for tensile and compressive loads in all directions. The detailed measurement methodology is described in Ref. [26]. The results were interpolated and graphically displayed over the workspace. Large nonlinearities regarding static compliance values, as well as a non-symmetric distribution of these to the robot's x-axis have been measured experimentally. Fig. 3 shows the static compliance values in the y-direction (described in detail later in Fig. 11) for loads in that direction. In this plane, the measured static compliance rises with the x-coordinate. The values at negative y-coordinates are lower than at positive y-coordinates.

Fig. 4, in contrast, shows the distribution of the static compliance in the x-direction of the xz-plane for loads in the x-direction for an exemplary result. The maximum static compliance values in this case are located in the middle of the workspace. Overall, the lowest values have been measured for loads in the x-direction and the highest for loads in y-direction.

Please cite this article in press as: A. Verl, et al., Robots in machining, (2019), https://doi.org/10.1016/j.cirp.2019.05.009

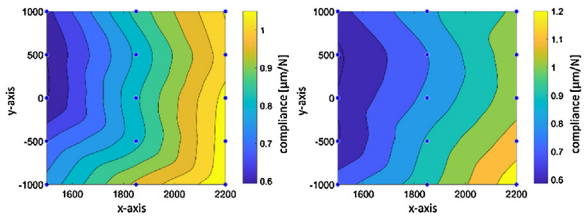

Fig. 3. Static compliance values in y-direction in the xy-plane (z = 900 mm) for tensile (left) and compressive (right) loads in the y-direction; x and y axes in [mm], respectively.

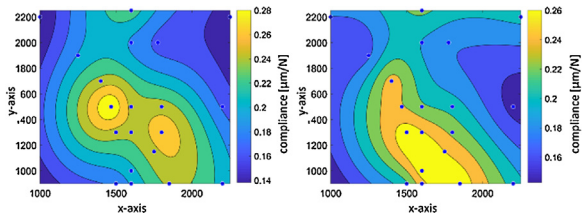

Fig. 4. Compliance values in the xz-plane (y = 0 mm) for tensile (left) and compressive (right) loads in the x-direction; x, y axes in [mm] respectively.

According to Karim et al. [27], the preferred feed direction for machining tasks should therefore be in y-direction to minimize deflections of the TCP from the commanded path. Although differences between static compliance values for tensile and compressive have been measured, the variation is negligible. The measured values for the Cartesian static compliance were used to calculate the joint compliance values for all six robot axes robot using the approach from Ref. [28]. The results are shown in Fig. 5.

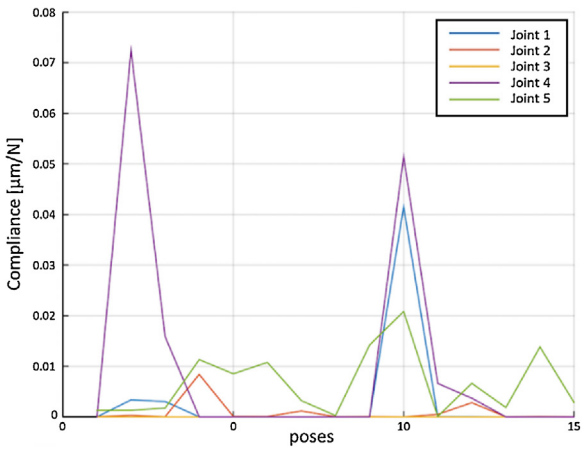

Fig. 5. Calculated joint compliance values.

The measurement protocol and the pose description can be obtained from Ref. [28]. The calculated joint compliance values exhibit a strong dependency on the pose (position and orientation of the TCP). For instance, the calculated joint compliance for joint three is almost zero in general, but in some poses, the value represents the overall maximum of all calculated values.

Because of the distinct pose dependency and the significant differences for loads in different directions model-based approaches, which are presented in many research projects to determine the robot's static compliance behavior, can only be considered valid in a small area. It is shown that such models need to include effects such as nonlinear friction and backlash, the influence of possible gravity compensations as well as differences for all load directions. Even though the determination of these effects results in a higher effort, an experimental determination of the static compliance values is necessary for describing the compliance behavior in a broader work area. Since each robot behaves differently this effort increases even more. However, laser scanners or laser vibrometers, as applied in Ref. [28], can be exploited in order to automate the measurement of numerous points on the robot's structure.

2.4.1. Static stiffness modelling and measurement

A key requirement for offline robot compliance-induced error compensation methods is knowledge of the robot stiffness. An example of measuring static stiffness comes from Cognibotics [29–31]. Their approach is that robot mechanics can be modelled and identified, and not just identified assuming stiff arm components. There are three areas to be modelled and identified: (1) arm kinematics, including individual variations due to differences in the tolerances and assembly of the arm components; (2) joint flexibilities including backlash and bending inside the gearbox; and (3) link flexibilities, including bending arm castings and bearings. Modern symbolic manipulation languages enable the creation of robot models which can be used in the next step: identification.

Lehmann et al. [32] used the internal measurement system of the robot arm, and torque data in one or more clamped positions in order to bend the robot arm under controlled and repeatable conditions. Data from controlled bending motions is used in their study to identify the parameters of an elasto-kinematic model of the arm joints, gearbox, and links. This model and data are then combined to identify the normal or stiff kinematic model of the arm. The remaining parameters are then found by relying upon specific measurement approaches. The final step is to apply this model to the machining process. This method performs a two-stage machining process. In the first stage, the elasto-kinematic model is not used, but the nominal robot parameters and programmed points are used to perform the first stage machining. In the second stage, the knowledge of the recorded process torques, motor angles, and the elasto-kinematic model allows an accurate estimation of the amount of tool-tip deflection that occurred during the process in the first stage. The tool-tip deflection is then used to modify the program target positions during the next and subsequent machining operations.

Another approach (Fig. 6) to measure kinematic and joint stiffness parameters was developed at the Advanced Manufacturing Research Centre (AMRC, University of Sheffield). Forces in two orthogonal directions and a moment can be applied on a robot in this setup. Deflections on the robot are measured with a laser scanner. After this identification, using the redundant degree of freedom in the robot, the joint configurations can be optimized for minimum compliance [33].

Fig. 6. Setup for identification of joint stiffness of a robot.

For example, the robot configuration with minimum compliance in X-direction is presented for a given end effector position and orientation in Fig. 7(a). Influence of the orientation is demonstrated in the color map in Fig. 7(b). The map compares the maximum compliance in x-direction on an xy-plane at a given z height and end effector position and orientation achieved by selecting the worst joint configuration and the minimum compliance achieved by the optimum joint configuration for the same end effector position and orientation. It presents the ratio of maximum to minimum compliance for the given xy-plane simulated between 1.6 and 2.6 in Fig. 7(b).

This demonstrates that using the redundant degree of freedom of the robot and a stiffness model, compliance of the robot in a

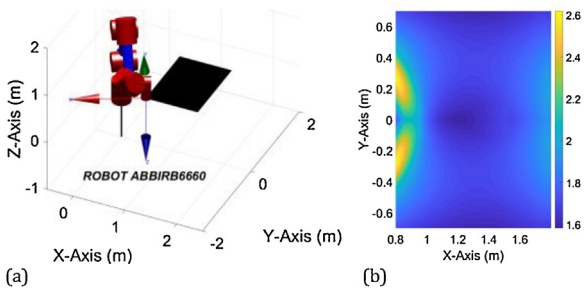

Fig. 7. (a) Robot configuration with minimum compliance in x-direction. (b) Ratio of maximum to minimum compliance in x-direction in the given 2D work space.

certain direction can be optimized and the improvement can be as high as 2.6 times. Work in progress aims to validate the improvements in this field experimentally.

2.5. Dynamic behavior

The dynamic behavior of an industrial robot is important for machining quality and accuracy. Especially for milling tasks, common use-cases in robot machining where high forces occur in a periodic manner, the robot structure's dynamic properties are critical to avoid severe oscillation and consequent machining errors. Oscillation amplitudes especially escalate when process forces match the robot structure's natural frequency and the direction of vibration modes.

Tunc and Stoddart [25] showed the dynamic stability of the robotic milling operation to be significantly influenced by the direction dependence of the frequency response functions (FRF) of the tool tip along the orthogonal Cartesian directions (x and y) defined relative to the robot base coordinates. Fig. 8 shows the oriented frequency response functions of a Fanuc F200iB 6-DoF (degrees of freedom) parallel kinematic robot as a function of the feed direction. They proposed an algorithm to determine the tool path (feed direction) that maximizes the dynamic stability of the machining operation. This work highlights the importance of accounting for the continuously varying tool tip dynamics when determining the most stable cutting conditions for robotic milling.

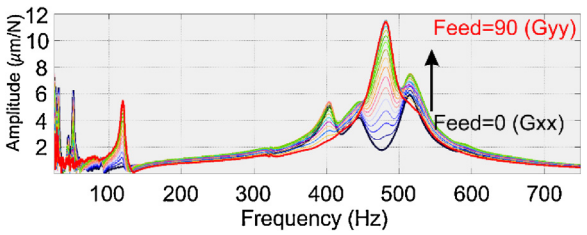

Fig. 8. Oriented FRF variation, Fanuc F200iB with feed direction [25].

Cen and Melkote [34] presented a stiffness model for the robot milling process based on the conservative congruence transformation (CCT). Their work is based on the recognition that the Cartesian stiffness of the robot is affected by the external force [35]. This, in turn, alters the robot geometry through the differential Jacobian, because of the elastic deformation of the joints and links. By adjusting the cutting parameters, it is possible to reduce the angle (γ) between the external force vector and the maximum principal stiffness vector (K_{max}) of the robot thereby enhancing the dynamic stability of the machining operation. Fig. 9 schematically illustrates the approach and the dependence of the stability boundary as a function of the cutting parameter (tool feed in this example). The authors demonstrated the suppression of mode coupling chatter in robotic milling experiments conducted on a KUKA KR210 industrial robot [34].

In another work, Lienenlüke et al. [36] introduced an expert system with a static compliance model that is trained with process data to link process planning parameters with process behavior. To

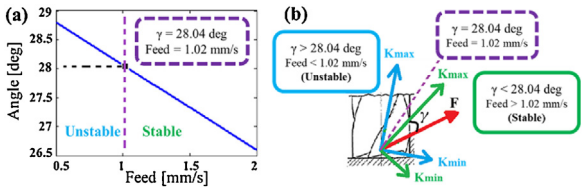

Fig. 9. (a) Effect of cutting parameter (tool feed) on dynamic stability angle, (b) Schematic illustration of stability enhancement principle [34].

optimize machining results, the expert system recommends cutting parameters to plan the process.

Using experimental modal analysis, Mejri et al. [37] have characterized the variation in the FRF of the tool tip as a function of vibration direction and robot position (or robot pose) for an ABB IRB 6660 industrial robot equipped with a high-speed machining spindle. For a given robot pose, they found that the modal frequencies in the two orthogonal directions of excitation can be different. Fig. 10 shows a typical result for the real part of the FRF, which governs machining dynamic stability. They also found that the robot was more stable when machining in the y-direction than in the x-direction, per their convention.

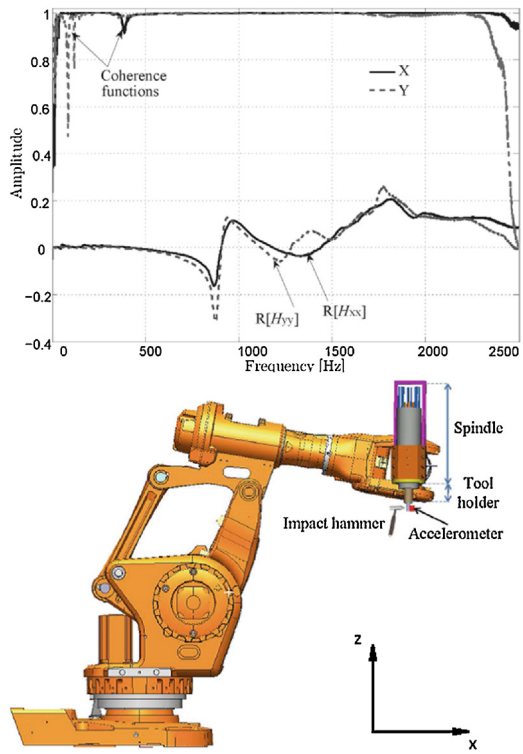

Fig. 10. Variation in the FRF (real part) of the robot tool tip as a function of excitation direction(top) for an ABB IRB 6660 robot (bottom) [37].

To identify the detailed dynamic behavior, like natural frequencies and modes of a structure, an experimental modal analysis (EMA) can be performed as was the case in Ref. [38] on a KUKA KR 500-3 MT "machine tooling" robot. The basic concept of an EMA is to compare a force of excitation with the reaction of a structure and compute a transfer function. Hereby modal parameters such as natural frequency and mode shape, which describe a structure's natural oscillation, can be determined. While the excitation in Ref. [38] took place with an impact hammer at one point close to the TCP, the response was measured with accelerometers on 63 points spread out across the structure and in all three directions x, y and z. This allows insight into the oscillation of all robot parts. Since the tests were focused on the direction- and pose-dependency of the dynamic behavior of the robot, the structure was excited in two directions, y and z (x did not show different modes in preceding tests). Experiments were performed in 23 different poses within the robot's workspace. Joint

configurations included fully stretched out as well as retracted poses. Evaluation of the data showed recurring mode shapes in all poses.

Fig. 11 shows the manipulator deformation in the first mode. Segments are color coded for increasing comprehensibility. The robot's first axis (green) is the joint responsible for the oscillation that occurs at frequencies between 5.8 Hz and 8.1 Hz depending on the pose. The second mode showed the manipulator pitching between 8.5 and 12.3 Hz, caused by a tilt of the first axis' bearing.

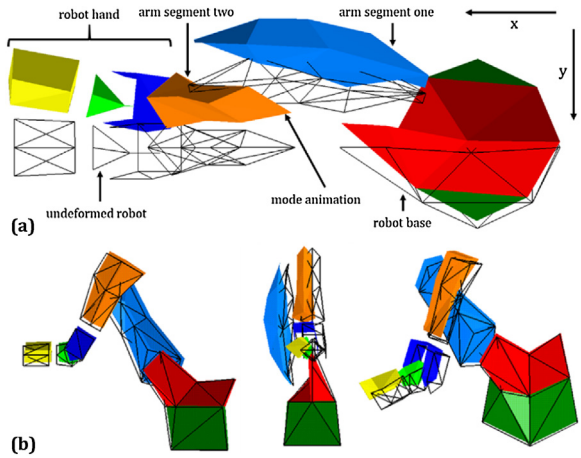

Fig. 11. Robot arm deformation in the first oscillation mode. Robot top (above) and side views (below), respectively.

Fig. 12 shows a linear interpolation of the natural frequency of the second mode as a function of the TCP position. Black dots mark the measurement points. Higher modes at higher frequencies show more complex shapes and movements of axes three and four [38]. The value of the natural frequencies changed with different TCP positions. In general, the more stretched out the manipulator was, the lower the measured frequencies were.

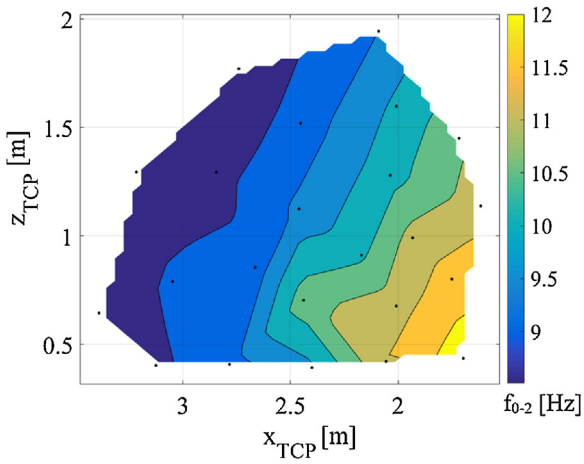

Fig. 12. Second natural frequency as a function of the TCP position.

The results show a high pose-dependency of the robot's dynamic behavior and different oscillation directions at different frequencies. This suggests a high dependency between the process execution and the machining quality. This is confirmed for milling experiments [27], additionally showing an impact of up to six modes on the process, unlike conventional machine tools, where only the first few modes are relevant. Further investigations have been conducted to exclude that these vibrations were caused by the workpiece itself, the fixture or the tooling. In order to exploit a machining robot's full potential, the dynamic behavior of the system has to be well known. This way, tasks can be carried out in the optimal pose and feed direction for a specific system. Critical configurations can be avoided to minimize dimensional and surface quality errors.

For robot machining applications, this means that further experiments with different robots have to prove whether the qualitative dynamic characteristics of all serial six-axis industrial robots are similar to the results of Ref. [34]. Research results also suggest that the robot's joints are the major cause for oscillations when using off the shelf robots for machining.

2.6. Path planning methodologies

Path planning is usually optimized considering two main objectives: reduced processing time and smoother trajectories. In the first case, the goal is to minimize the time necessary to execute a certain trajectory in order to match productivity requirements [39,40]. In the latter case, a path quality index is favored and time is treated as a constraint [41]. Some optimization methods consist of a mixture of the aforementioned ones, proposing a trade-off between execution speed and quality. In Ref. [42] some of these approaches are compared taking the execution time and the norm of jerk into consideration. Since the specific kinematic structures of many commercially available robots induce uneven distributions of workload on motion axes, the efficiency and quality of trajectories is not necessarily a by-product of a geometrically optimal path planning. This aspect is important not only for machining segments of the tool path but also for rapid movements, where optimized trajectories could improve overall lead-time and reduce structural stresses.

Various studies focusing on these topics rely upon the use of piecewise splines, whose coefficients are optimized using different approaches. For example, in Ref. [43] a B-spline representation of trajectories is used, and a function that concurrently considers both the total execution time and the minimization of the norm of jerk. Depending on the nature of the chosen objective function, the optimization approach may range from the classical resolution of a quadratic programming problem to the minimization of a highly non-linear functional. In this case, general-purpose optimization approaches must be adopted, like in Ref. [44], where the norm of jerk for the robot joints is minimized numerically by a genetic algorithm. A similar approach is proposed also in Ref. [45], but in this case, the chosen objective is a function of manipulability measures and thus involves inverse kinematics.

As mentioned before, process efficiency and quality may also be improved by optimizing rapid movements. In these cases, authors target the planning of smooth trajectories in the Cartesian space, while downgrading the speed of all joints based on the slowest one [46] and on achieving a higher degree of regularity by increasing the polynomial degree of the path or of the motion profile [47–49]. Multiple-axis movements are often managed in the operations workspace [50], although the definition of trajectories in joint space is, in some cases, a viable simplification that allows the implementation of smoother joint trajectories [51]. A different approach is implemented in Refs. [52] and [53], where kinematic quantities are optimized in the joint space, based on a sine-jerk model for joint motion profiles, and the dynamic characteristics and limits of each joint are considered to enable an even distribution of workload along the kinematic chain. Manufacturing applications in which the robot is subjected to continuous, potentially strong excitations, for example, cold spray [54], could also benefit from path planning strategies that consider the stiffness variation across the whole task space. Mekaouche et al. [55] present a finite-element-method-tool for mapping robot structure stiffness over the work space for a generic kinematic chain.

2.7. Control

A robot controller is usually a processor-based electronic or a standard personal computer (PC) device that can be programmed to drive the motors attached to each robot axis and coordinate their

motion while ensuring that the TCP executes specific trajectories with assigned motion profiles [56]. Such trajectories are generated at the CAM level and then fed to the robot CNC in the form of a part program.

The controller can additionally command the digital and analog input and output (I/O) signals to command external devices, such as a cutting tool or a welding gun, based on a sequence synchronized with the robot motion. Such signals are sampled with cycle times related to the application. The robot controller communicates with other controllers or PCs and uses sensors to obtain information about the robot environment, in order to modify the robot tasks accordingly. For example, images coming from vision sensors are typically streamed to an external PC that is connected to the CNC. These images are therefore processed outside the controller: specific information is elaborated on the PC and collected by the CNC with a sampling cycle time related to the process dynamics (from 5 to 150 ms).

When available in the CNC, the timing associated to the actual implementation of the adapted information is enabled in the part program by integrating targeted check points during its execution. Fig. 13 outlines the major components of a robot CNC.

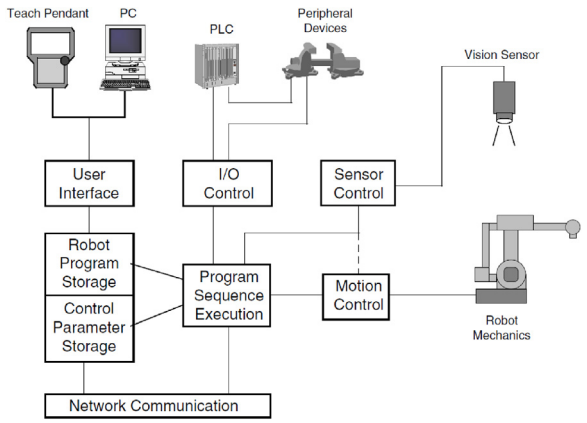

Fig. 13. Robot CNC architecture.

The trajectory strategy behind robot motion control aims at obtaining high quality products and robust processes [57]. This frequently demands the robot CNC to embed the process model and a set of process key performance indicators (KPIs) that can be tracked over time and space. Based on these *observed KPIs*, specific process optimization strategies can be implemented. The following section provides an overview of typical process control strategies in machining robots.

2.8. Process control strategies

A literature review of process control strategies for robotic machining reveals two broad approaches to minimizing the sources of error and process instability. The approaches consist in offline and online methods. Robots are currently used more often in milling [22] and drilling [58–60] especially for large parts, molds and dies. They offer easier set-up and portability than large machine tools, but are significantly less stiff than these, hence they cannot be used in all machining applications. The following approaches outline some of the opportunities to boost the adoption of robotics in machining tasks.

2.8.1. Offline methods

Offline error compensation strategies seek to minimize the effect of non-kinematic error sources such as robot joint and link compliance on the robot positioning accuracy, and in turn, the machining error, through optimal selection of the robot configuration, machining direction, and cutting conditions during tool path generation using improved static or dynamic models of the tool-workpiece interaction.

The procedure of Klimchik et al. from Refs. [61] and [62] is illustrative of the general strategy used for offline compensation (Fig. 14).

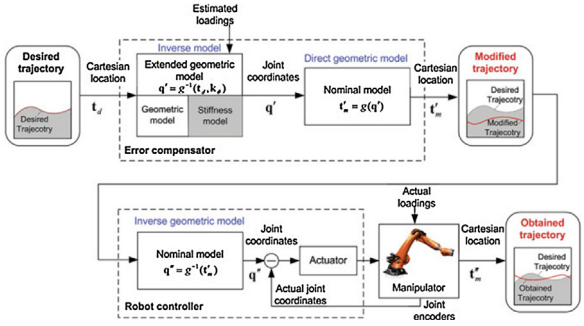

Fig. 14. Offline process control strategy [62].

A predictive model is used here to estimate the machining forces anticipated along the nominal machining trajectory necessary to produce the desired part feature. These are then input to either a static or a dynamic compliance model of the robot to compute the optimum joint configurations that will yield the desired Cartesian positions of the robot tool tip in the presence of the machining forces. The nominal robot configurations along the tool path are then modified, based on the optimized joint configurations, to obtain the modified trajectory, which is then fed to the robot controller for execution using the forward kinematics model contained in the robot control software.

Klimchik et al. [62] developed and implemented the offline compensation strategy on a KUKA KR-270 industrial robot with six degrees of freedom (DoF). They utilized a time-domain simulation of the dynamic milling forces using the approach of Altintas [63] to compute the instantaneous milling forces, which were used to determine the robot configurations that minimize the compliance induced errors along the desired trajectory using an iterative numerical approach. Their experimental results demonstrated >90% reduction in the maximum deviations of the tool tip due to low frequency (7 Hz) robot compliance in the presence of milling forces. While this result is promising, their work does not address reducing machined surface errors caused by higher frequency vibration modes that can be excited by periodic milling forces.

As part of the EU FP7 COMET project, Schneider et al. [64] developed an offline error compensation strategy based on a detailed investigation of multiple error sources in robotic machining. They proposed a modular approach to overcome accuracy issues either in offline or online. Their study was another example of how laser trackers can be used in real-time position compensation for machining robots together with an additional piezo actuator based high-dynamic compensation mechanism. The authors also analyzed several sources of error such as backlash, static and dynamic friction, and nonlinearities in joint stiffness [65] and incorporated these effects in their offline compensation approach. Dimensional errors as low as 0.05 mm were obtained in pocket milling tests on aluminum. In more recent work, Diaz Posada et al. [66] presented their offline error compensation strategy (Fig. 15) with experimental verification results obtained on a KUKA Quantec KR270 2700 industrial robot.

Fig. 16 shows representative improvement in circularity error obtained through offline compensation of cutting force induced compliance of the robot TCP when milling a circular contour in an aluminum workpiece. Similar tool tip error offline compensation strategies have been reported by other researchers [67–69].

In robotic machining, the presence of kinematic redundancy enlarges the workspace of the robot and increases the number of feasible robot configurations (poses) for machining the desired feature. For example, using a 6-DoF robot to perform a 5-DoF machining task yields a first-order redundancy. Since robot Cartesian stiffness varies with configuration, redundancy resolution techniques [71] can be utilized to derive stiffer robot poses,

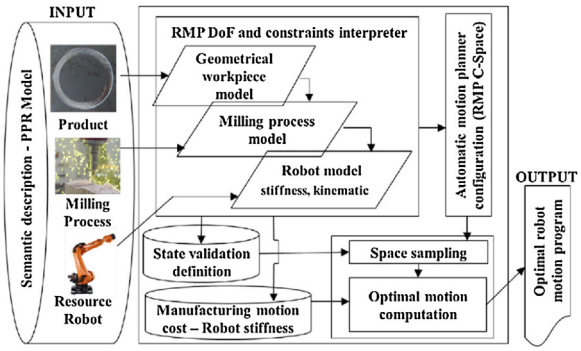

Fig. 15. Offline compliance error compensation approach [66].

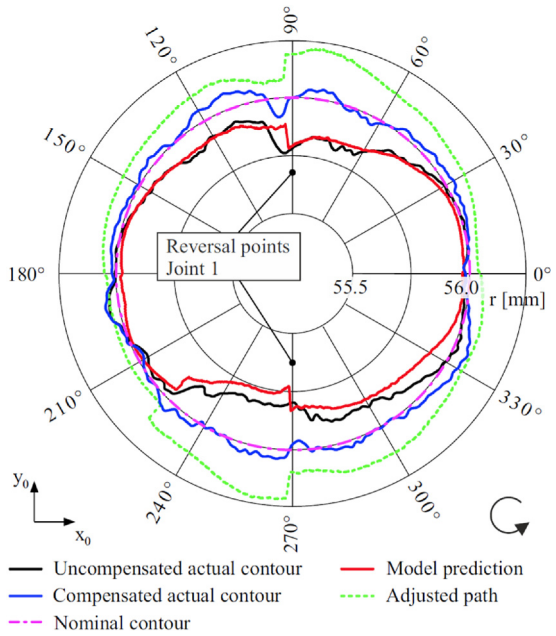

Fig. 16. Improvement in circularity during robotic milling of aluminum through offline adjustment of tool path by compensating for joint stiffness and joint hysteresis induced errors [70].

thereby enhancing the machining accuracy. Practical examples of redundancy in robotic systems include a robot mounted on a linear track, mobile platform, or overhead gantry robot. Fig. 17 shows an example of a milling robot on a mobile platform designed for high accuracy machining of large aircraft structures. Such systems are being actively researched for industrial applications, particularly in the aerospace industry.

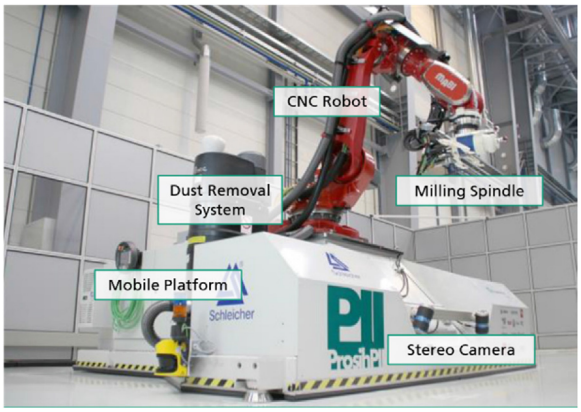

Fig. 17. Mobile milling robot: machining of large aerospace structures [72].

Andres et al. [73] utilized a redundancy resolution method based on minimization of a position-dependent scalar performance index that seeks to keep the robot pose away from ill-conditioned poses and away from joint limits. Experimental assessment of their redundancy resolution method was conducted on a KUKA manipulator for milling a relatively soft polymeric material. Xiao and Huan [74] have also proposed different criteria based on singularity avoidance, joint limit avoidance, and collision avoidance for use in resolving kinematic redundancy in 6-DoF industrial robots used for machining tasks.

Sabourin et al. [75] presented a kinematic redundancy-based path planning optimization method to enhance the machining performance. They discussed and analyzed a number of different criteria including kinematic, mechanical advantage, and stiffness to improve various performance metrics of the robot for a machining task. Work cells with a 9-DoF serial link manipulator and a 11-DoF parallel kinematic machine, respectively, were analyzed using various redundancy resolution criteria.

Mousavi et al. [76] studied the effect of one and two degrees of functional redundancy on the dynamic stability limit (for chatter vibration) in robotic milling. Fig. 18 shows an example of the effect of two functional degrees of redundancy arising from the presence of a rotary table and the rotation of the tool about its axis on the stability limit defined by the depth of cut.

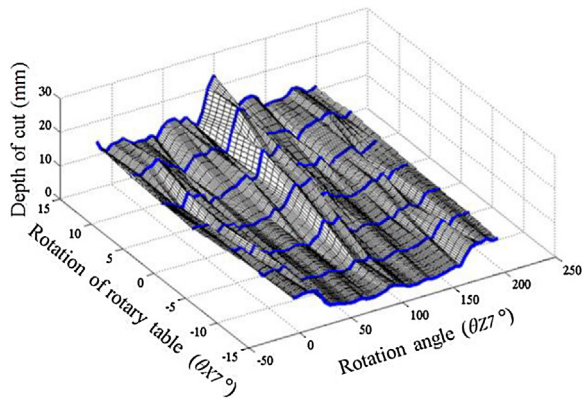

Fig. 18. Effect of 2-DoF functional redundancy on the chatter stability limit in robotic milling with an ABB IRB6660 industrial robot [76].

In addition to model-based methods to compensate for robot compliance induced machining errors, work on model-based methods to suppress the onset of dynamic instability in robotic machining operations has also been reported. While chatter vibration in machining with CNC machine tools is typically characterized by higher frequencies [64] and is usually due to chip regeneration, the low and comparable stiffness values in the principal stiffness directions of the robot [77] give rise to mode-coupling chatter, which typically occurs at much lower frequencies (10–20 Hz) [78].

It is evident from the literature review on offline methods for robotic machining process control that much work has focused on developing model-based methods designed to minimize robot-compliance-induced machining errors and/or to suppress dynamic instabilities through modification of the tool path, optimization of the robot configuration (with or without kinematic redundancy), and modification of cutting parameters. A rigorous analysis and comparison of the different offline compensation and chatter suppression strategies should be developed based on this.

2.8.2. Tool path accuracy

Tool path compensation in robotic milling has been an active research area in the last decade. In literature, the major sources of robot compliances have been identified as the gears and bearings at the link joints [19,79,80]. Offline tool path correction is the simplest approach, especially for high volume parts, where repetitive part measurements by coordinate measurement machines are involved [81]. However, this method may not have economical merits, especially for large-scale parts targeted by robotic milling. Considering this, methods based on robot stiffness modelling have been the focus in the literature.

Belchior et al. [82] applied robotic offline tool path correction on progressive sheet metal forming process. Barnfather et al. [83] proposed to use photogrammetry assisted robotic machining to compensate inaccuracies in robotic milling of two stage processes. The closest point to the nominal cutting frame on aligned inspection surface is used as a base for compensation. Then, the surface dislocation errors generated in the previous pass are compensated during the finishing pass. It was demonstrated that accuracy can be increased by using photogrammetry assisted compensation. In milling of circular pockets, the diameter error was decreased from 500 μm down to 200 μm, whereas cylindricity error was improved from 1000 down to 250 μm.

Zäh and Rösch [84] proposed fuzzy logic-based controllers to improve the tool path accuracy in robotic milling by compensating the static deflection of the robot during robotic milling process. In some applications where increased stiffness is required, 6-axis parallel kinematic robots are used [85,86]. A drawback of such solutions is the need for extensive experimental calibration.

In an early study on real time correction of the robot position in robotic milling, Zhang et al. [87] investigated major topics and approaches. They proposed real time compensation of robot deflections and improved the process performance in terms of accuracy. The results in their study were revolutionary and showed that robots can exhibit high performance milling through real time path compensation techniques. Recently, laser tracking systems, contrary to their high capital investment, have started to be used in tool path correction for robotic milling applications.

In a later study, Shi et al. [88] used a 3-axis laser tracker for real time tool path correction. They focused on linear and circular type tool path geometries, where major improvement was achieved in tool path accuracy from 2 mm levels to the order of 50 μm.

The second major obstacle in the integration of industrial robots in milling processes is the low frequency modes introduced by their flexible structures. High amplitude vibrations that occur at low frequencies subsequently result in high fluctuations in the cutting forces. As a result, part surface, tool body, spindle and robot axis can be damaged.

Addressing dynamics and stability of robotic milling, Pan et al. [18] were the first to demonstrate the deep marks left on the part surface by the robot vibrations in robotic milling. Zaghbani et al. [89] applied a variable spindle speed strategy for vibration control and minimization in robotic milling, where they used the cutting force and vibration data as a measure of stability in their statistical approach. It is shown that spindle speed variation can be used as a chatter mitigation strategy in robotic milling.

Tunc and Shaw investigated the effect of the flexible robot structure on dynamics [85] and stability [86] of robotic milling while machining AL7075 and AISI316L type materials. In their first study, a Stewart type hexapod platform was utilized for robotic milling. The dynamic response at the tool tip and the hexapod platform were measured using impact hammer tests. It was demonstrated that the robotic platform can introduce low frequency modes which may be as flexible as the cutting tool modes. The position and direction dependent dynamics introduced by the robotic platform have been clearly shown, as well. With regards to the effects of robotic platform on milling stability, they demonstrated three fundamental aspects, i.e. position dependent stability, effects of cross transfer function on stability diagrams and the role of feed rate direction on the stability lobes, and absolute stability limits due to the asymmetrical dynamic response at the tool tip, which means that the measured frequency response function (FRF) along feed (x) and cross feed (y) directions are different from each other in terms of both amplitude and natural frequencies of the dominant modes (Fig. 19). They also demonstrated the effect of tooling to minimize position dependency of stability diagrams. The cases were handled in two main groups, where the stability was governed by the robot structure and the tool modes. Simulations and experiments were used to show that, for the cases where radial depth of cut is less than 50% of the tool diameter, the cross-transfer functions may significantly affect stability diagrams.

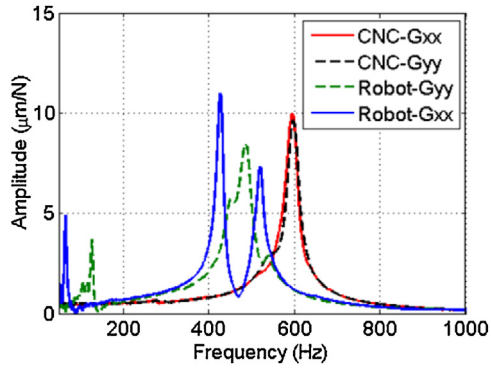

Fig. 19. Demonstration of asymmetrical and symmetrical tool tip FRF in robotic milling and CNC milling, respectively [86].

In a recent study, Maurotto and Tunc [90] investigated the effects of low frequency chatter introduced by the robot structure on surface integrity in milling of Inconel 690 by comparing the surface residual stress and surface roughness in different chatter conditions. They showed that the low frequency chatter governed by robot modes increases the magnitude of the residual stress by about 40% compared to cases where dynamics is governed by the tool mode. The standard deviation of surface residual stress also increases.

2.8.3. Online methods

This section reviews online process control strategies employed to improve the accuracy of robotic machining operations. The basic approach in online strategies is to utilize sensor feedback to directly measure the robot end effector position or indirectly estimate the machining error and compensate for it in real-time using an appropriate control algorithm. Early efforts aimed at implementing sensor feedback-based control of industrial robots in high force machining tasks (e.g., force controlled grinding or deburring) revealed significant limitations in the bandwidth of the robot motion control loop. To address this problem, researchers at Lund University in Sweden developed hardware and software extensions to an ABB S4CPlus control system to enable the integration of external sensors and control algorithms based on real-time sensor data [91]. Fig. 20 shows the extended control architecture, which enables external sensor-based feedback control at the task, joint, cartesian, and motor control current levels. Using this architecture, modification of the servo arm-control commands at sampling intervals of 4 ms were realized.

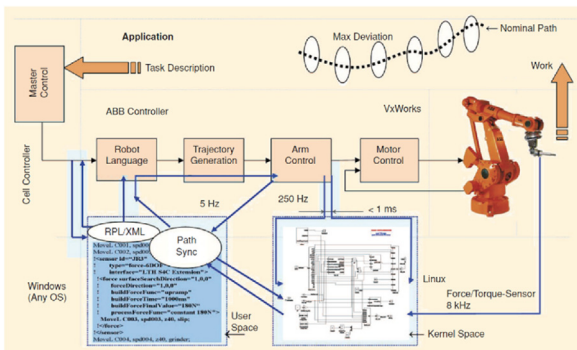

Fig. 20. External sensor-based feedback control architecture [91].

Bottero et al. [92] analyzed the compensation for periodic torque disturbances, characteristic of electrical permanent magnet motors. The compensation was obtained as a two-stage adaptive controller. The final compensator was then obtained via a pure predictive feed forward compensation with an internal model of the disturbance. The stability and robustness properties of the overall adaptive compensation technique could then be experi-

mentally validated on industrial manipulators. Today, industrial robot controllers come with external sensor interfacing features (e.g., KUKA RSI [93]) that enable real-time communication between robot controller and external sensors.

Olsson et al. [94] developed a control architecture to implement force-controlled drilling of flexible aircraft skin material on an ABB IRB 2400 IR. A 6-axis force/torque sensor was used to measure the x–y–z forces and torques produced in drilling. A dynamic model of the robot response to external forces and moments was used to design a feedback/feedforward control algorithm that adjusts the clamp-up force of drilled sheets in real-time. Evidence of reduced x–y tool deflections was shown, but no direct improvement in hole quality was found. Pan and Zhang [95] implemented a hybrid position and force control scheme in an ABB IRC5 robot controller to improve robotic milling accuracy. An ATI 6-axis force/torque sensor was used to measure the milling forces in real-time, after compensating for the spindle and tool. Fig. 21 shows the force control loop utilized in their work. Corrections were made to the robot's nominal position and velocity via the trajectory generator. The authors implemented real-time robot deformation compensation and reduced workpiece surface error.

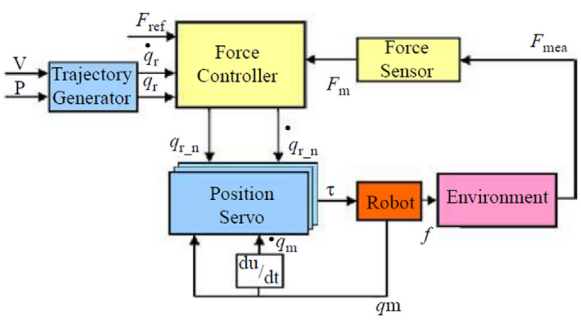

Fig. 21. Force control loop implemented in an ABB IRC5 controller [95].

Schneider et al. [96] used a series of LEDs and three cameras (Nikon K600 metrology system) to track robot end effector and compensate in real-time the error in position by modifying the joint servo commands based on the measured position error. Using a PID control algorithm, end effector position control of a KUKA KR125 IR was achieved at 500 Hz, acceptable for IRs.

Fig. 22 shows the machining error obtained with the position error control strategy when milling a circular slot in a steel workpiece. Profile accuracy improvement of over 46% was reported by the authors of the studies presented in Ref. [96].

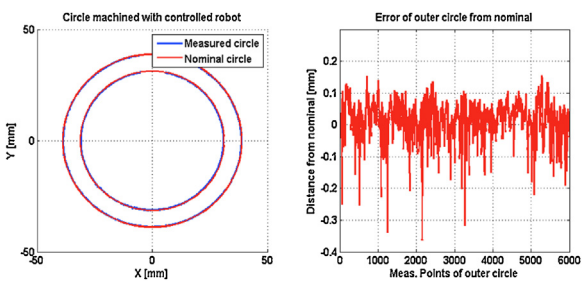

Fig. 22. Machining error using a tuned PI control algorithm based on real-time end effector position sensing [96].

Later work by Schneider et al. [97] extended their real-time position error compensation approach to include a combination of macro and micro manipulation. A KUKA KR125 industrial robot was the macro-manipulator used to hold the workpiece, while a 3-axis translational piezo-actuated system served as the high bandwidth micro-manipulator on which the milling spindle was mounted. A parallel-link flexure mechanism enhanced the dynamic properties of the piezo-actuated micro-manipulator and to extend the range of compensation in each axis to 0.5 mm. The robot position and orientation in the workspace was measured at 440 Hz using a metrology system. Fig. 23 shows the system architecture.

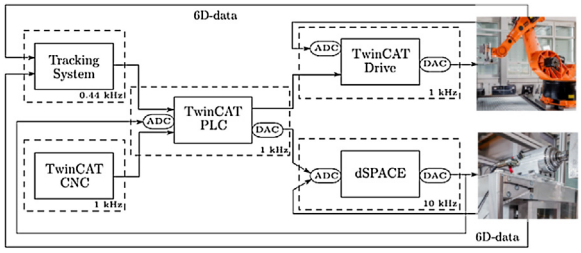

Fig. 23. Overall system architecture of the combined macro and micro manipulator actuated system [97].

Subsequently, Fig. 24 shows measured profile errors obtained in machining a circular slot similar to Ref. [96]. The authors indicate that machining accuracy of ±100 μm can be obtained with the combined macro and micro-manipulator system in milling of steel.

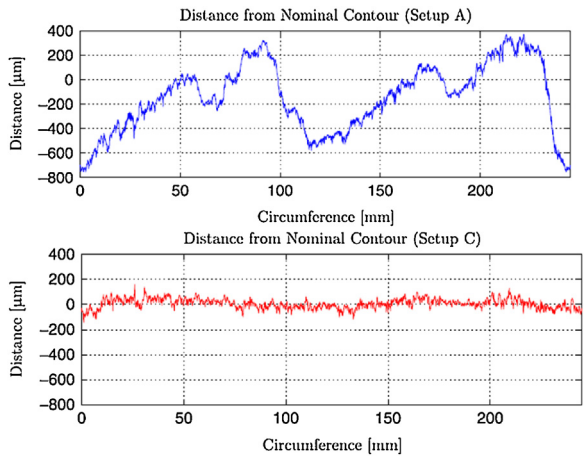

Fig. 24. Deviation of the machined outer circle, measured using a coordinate measurement machine. Setup A: only position-control of the robot. Setup C: micro and macro manipulation including optical tracking, adapted from [97].

Diaz Posada et al. [98] investigated the improvement in robot positioning accuracy in robotic drilling using a 3D laser tracker to compensate for the end effector position and orientation errors, and a robot compliance model-based compensation implemented in the external controller interfaced with the robot controller. Their results show the laser tracker-based compensation is able to reduce the translation errors to less than 0.1 mm and keep rotation errors to a maximum of 0.2° in robotic drilling of metal sheets.

Work on real time pose control of an industrial robot using 3-DoF and 6-DoF laser tracking has also been reported by Moeller et al. [99]. Fig. 25 shows the positioning path accuracy (AT_p) and the repeatability error (RT_p) obtained using external closed loop control based on the laser tracker data. It can be seen that there is significant reduction in the AT_p parameter with 3- and 6-DoF control but the improvement in repeatability error is not significant. However, the external control approach outlined by Moeller et al. is shown to produce considerable reduction in the

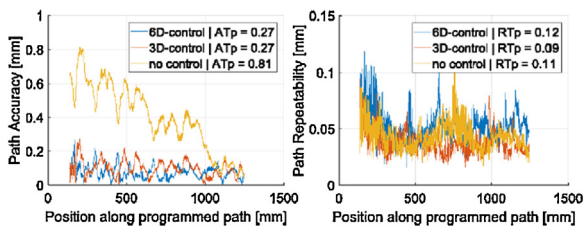

Fig. 25. Path positioning accuracy and robot repeatability error with and without laser tracker-based control [99].

robot deflection induced error produced in machining polyurethane material.

Cen and Melkote [100] recently presented a wireless force sensing based approach to compensate for robot positioning errors in robotic milling, summarized in Fig. 26. A low-cost polyvinylidene fluoride thin-film force sensor developed in prior work by the same group was used to measure the milling forces in real-time. The measured forces are fed to a well-established mechanistic force model for end milling to compute the instantaneous radial and axial depths of cut, which gives the actual position of the tool relative to the workpiece. The error in tool position is then compensated in real-time by commanding the robot to the corrected position.

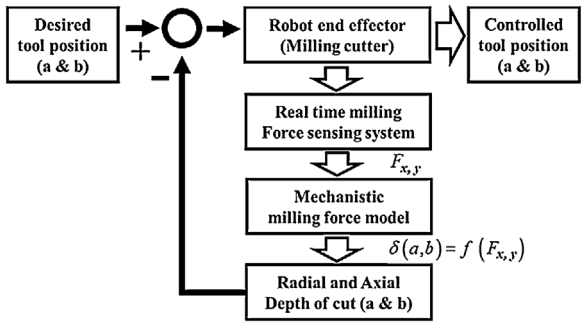

Fig. 26. Milling force model and wireless force sensor-based feedback compensation method [100].

The approach was implemented on a KUKA KR210 industrial robot and peripheral end milling tests were conducted at different feed rates. Fig. 27 shows the surface error obtained without sensor feedback-based compensation and with compensation. It can be seen that with sensor feedback-based control, the surface error is reduced by over 70%.

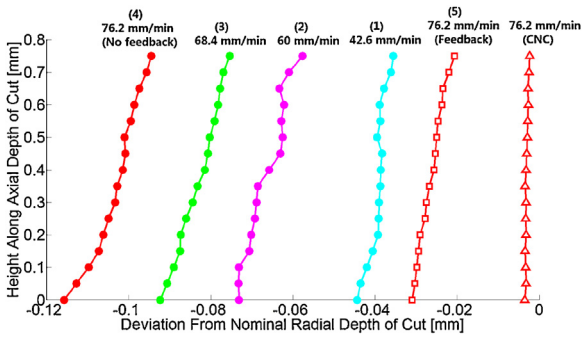

Fig. 27. Surface error reduction in a straight peripheral end milling cut using force sensor-based feedback [100].

Figs. 22, 24 and 27 provide quantitative examples of the reduction in machining error using online compensation strategies reported in Refs. [96], [97] and [100], respectively. It is evident, though, from the literature review on online process control strategies that there is room for further improvement in robotic machining accuracy through sensor feedback and control. This is an area of ongoing research in the community.

2.9. Robot temperature compensation

While the repeatability of standard industrial robots is satisfactory for many applications, their absolute accuracy is not sufficient for machining tasks or robot-based measuring systems. Manufacturing inaccuracies in robot production can often be permanently compensated by a one-time calibration, while drift effects, for example, due to wear or temperature, must be periodically compensated. In particular, the heat input of the drives combined with temperature fluctuations in the environment lead to relevant volumetric expansions in the structural components [101].

Due to the open kinematics of serial-link-based robots, unlike compact machine tools, expansion errors continue to accumulate from the base upwards. The problem is worsened by the uneven temperature distribution and by the different materials of the robot arm, which lead to tensions throughout the components [102–106]. The resulting displacement contributes significantly to the position accuracy errors [103]. There are various approaches to compensate for the effects of temperature-related deviations. The procedures generally follow the scheme in Fig. 28.

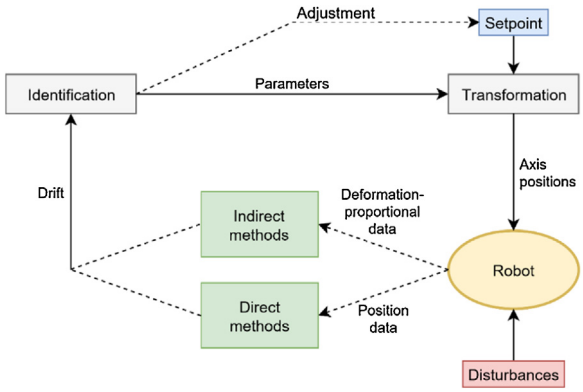

Fig. 28. General procedure for the drift calibration of robots [acc. to 106].

First, the drift deviations are determined from measurements on the robot. This can be done in two different ways: directly and indirectly. Based on this data, certain parameters are adapted. A distinction can be made between changing the target points in the robot program and internal adjustments to the path planning component of the control. The first option has the advantage of being robot-independent and does not require deeper access to its controller, but the temperature compensation must be considered individually in each program. The parameters of the transformation chain for calculating the inverse kinematics can be varied by optimization algorithms that can process identified position errors in such a way that the remaining errors are minimal [103].

The methods used for the determination of position errors can be divided into two categories: direct and indirect methods. Direct methods are based on the actual measurement of the position deviations of the robot arm, whereas indirect methods estimate the position errors from the measurement of quantities proportional to the displacement. Examples of such quantities are the change in length of individual components [104] or simply the temperature [102]. With the help of thermos-elastic deformation models, it is possible to calculate the displacement of the entire robot arm without additional hardware. In principle, these indirect methods are not as exact as the results of direct measurements, but the considerable cost advantage nevertheless makes them interesting for some applications [102].

The position measurement for one-time adjustment and calibration (after manufacturing) of industrial robots is usually carried out as part of a 6D calibration. In this calibration, spatially fixed measuring devices record the position and orientation of a measuring object attached to the robot, resulting in high fidelity data from some robot poses [107,108]. However, this method is only of limited applicability for the continuous calibration of robots. The reasons are: (1) the high cost of the measuring systems and of their installation location, and (2) a reduction of robot flexibility by mounting sensors close to flanges.

A 3D calibration is more practical in this regard. In this method, the measuring device is mounted on the robot and the measuring body is stationary. This method is simpler to integrate, especially in the context of robot-based measurement systems, where the robots are already equipped with measuring sensors. However, in contrast to the devices required for 6D calibration, the more compact sensors attached to the robot can usually only sense a position without orientation [109]. For this reason, a 3D calibration requires more robot poses to achieve similar accuracy [106].

In contrast to absolute calibration, drift compensation or relative calibration only uses a limited set of recent measurement values obtained at regular intervals. The robot approaches various targets on the measuring body and the sensors determine the position errors. On this basis, certain parameters particularly susceptible to temperature are optimized to minimize the position errors [101,103,105,106,109].

In a full calibration, all available targets are scanned and the compensation values calculated. This method is used after prolonged plant stops to compensate for substantial temperature changes. To avoid long pauses during operation, usually only a few targets are measured between the primary robot operations. These are subsequently used for calibration together with previously recorded measuring points, which is why the method is called split calibration [106]. In the primary application area of this technology, the robot-based inline measurement of components for quality assurance, the measurement results of the robot cells are compared with measurements from coordinate measurement machines in temperature-controlled environments at regular intervals. By adding offsets, the discrepancies can be further reduced.

3. Programming in robotic machining

Until recently, industrial robots were used in machining exclusively for loading and unloading, that is, for supporting machine tools in machining processes. But with the possibility of using them for machining tasks with low process forces, like chamfering or deburring [110], new requirements emerged for path planning and thus for the programming of industrial robots for machining operations. Some of the particularities of this field are presented in this section, along with practice examples.

3.1. Sensor based programming methods (deburring, polishing)

The application of a stereo camera system for external TCP-pose measurement increases the absolute positioning accuracy of an industrial milling robot by up to 0.1 mm [111]. For higher absolute accuracy up to 0.03 mm and error correction along the tool path during feed motion, dynamically measuring laser tracker systems are a suitable solution. External guidance (Fig. 29) makes the machining robot unsusceptible to external or constant process forces, thermal expansion and calibration errors [99].

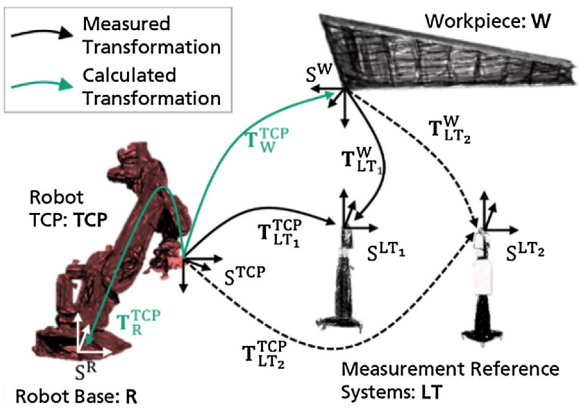

Fig. 29. External TCP-guidance and accuracy validation by two dynamic laser tracker systems [99].

3.2. Programming environment

Pre- and post-operations in machining, such as the determination of the workpiece's position and orientation as well as measurement of the geometry after machining, can be performed by robots using additional vision- and laser-based technologies. These operations can be executed using the robot control (RC). For the machining task itself, the RC has to be complemented with functions of a CNC, like in machine tools. Thus, the RC and its advantages can be used for pre- and post-operations but the path planning and trajectory generation for the machining part is done by the CNC. This is necessary because the RC is parametrized for the particular robot that it is commanding and hence, always machine-specific. CNCs, however, are used to ensure the proper machining of the workpiece [112]. The combination of RC and NC enables G-code programming of the machining process. Exploiting the flexibility of robots in machining G-code programming can be very complex and challenging. For this reason, the use of CAM-software is required to ensure simplified and collision free path generation.

3.2.1. CAD-CAM toolchain

The machining of components via CAM path planning usually starts by loading a CAD file into the editor of the CAM program. Various standard CAD data formats, such as STEP or IGS, can be read. After path planning (Fig. 30, Step2) the program can be exported in standardized or machine specific output formats.

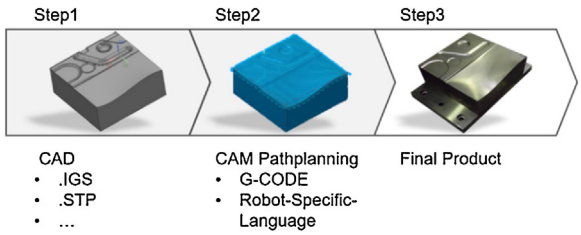

Fig. 30. Process chain CAD-CAM.

As shown in Fig. 30, the output format can be written into the respective programming language of the robot manufacturer or can be an output in G-code adapted for robot applications. The customized G-code may allow the use of a larger look-ahead, an extension of the program parser's look-ahead. Under these conditions more precise machining results can be achieved. Other possibilities of increasing the machining accuracy with offline programming using CAM tools are shown in Refs. [113–116].

In the project PROGEN [117], demonstrators of pressing tools were machined by robots. Processing was carried out on the same geometry with the same material. Path planning for the milling strategies was carried out using the same CAM program in G-code compilation, but varied in 3- or 5-axis programming. The results of the milling processes are shown in Fig. 31. The surface color is, analog to the scale, the deviation of the surface geometry in [mm] compared to the CAD design. The evaluation shown by a structured-light 3D scanner reveals that 3-axis machining has fewer geometry deviations over the entire component. This is mainly due to the frequent reorientation of the process head in 5-axis machining and the associated axis movement of the robot. The processing quality can be influenced by targeted robot poses [118] and skilled path planning [87]. In addition to the selection of optimal robot positions, the clamping position, the position of the tool path and the process-related technology parameters also determine the process result. Industrial robots with serial

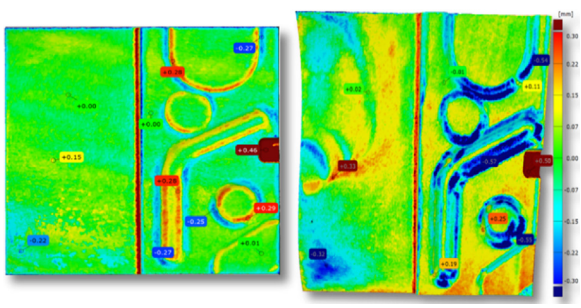

Fig. 31. Results of robot-based milling in 3-axis (left) and 5-axis programming (right) [117].

kinematics have a different static and dynamic behavior, depending on the process parameters [27].

Current CAM planning systems are unable to simulate static and dynamic properties of robot systems during process design. One approach was pursued in the publicly funded research project HORuS (at WZL RWTH Aachen) with a focus on integrating process behavior into process planning. The follow-up project HORuS^2 will further develop these findings. The main focus is on the development of planning assistance modules to increase the accuracy of robot systems for machining large components.

One exemplary module focuses on the reduction of inverse movements of the rotary robot axes during tool engagement. Studies have shown that inverse movements of individual axes lead to high path deviations [119]. Foresight or simulation of rotational axis movements during planning is currently only used for accessibility and collision checks, but not for analysis of critical inversion movements. Fig. 32 shows an approach for calculating rotational paths based on defined tool paths. It is possible to visualize critical areas and to adjust process parameters or machining strategies manually or automatically.

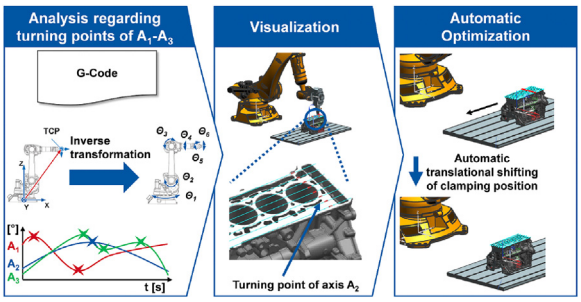

Fig. 32. Calculation of critical turning points of the rotational robot axes for reducing path deviations.

3.2.2. Dedicated programming possibilities

The robot control can be complemented by CNC functions to make sure that the robot can follow the desired and programmed path given as robot-specific languages and generated by CAM-software. This requires a particular architecture, discussed here by means of the KUKA.CNC.

KUKA is so far one of only a few manufacturers providing an integrated NC kernel. There are other examples for that such as the Siemens NX Robotic Milling Module, the announced COMAU Robot CNC control, or a similar solution from Stäubli. Another possibility, also from KUKA, is to combine CNC and RC. This is achieved with a Siemens 840D controller, the KUKA.CNC Sinumerik. This is a KUKA-specific development, to ensure accurate and improved path-behavior for machining tasks, because in this case, interventions on a low level of the RC are required. If such options are not available, the CAM software has to compile the programs into robot language, as described in Section 3.2.1. Thereby, the achievable machining quality is strongly dependent on the post-processors implemented in the CAM software. This is why a combination of RC and CNC should be favored, since offline post-processors do not have a feedback of the actual trajectory, whereas the RC does. Fig. 33 illustrates how RC (orange boxes) and CNC (blue boxes) interact within the KUKA.CNC.

The main tasks of a CNC are the calculation of numerous support points and the assurance of suitable path-dynamics, for example, constant velocity of the TCP, which in turn equates as the feed rate of machine tools. In order to provide these necessary functions, the CNC requires high computational power, since the path dynamics are dependent on the total movement and thus the high number of support points have to be considered by an enhanced look-ahead functionality for the actual path-generation. Therefore, such calculations have to be performed in real-time.

In conclusion, the RC is used to take advantage of robot-specific functions such as singularity avoidance or specific transformation algorithms. The RC-CNC combinations support the use of G-code

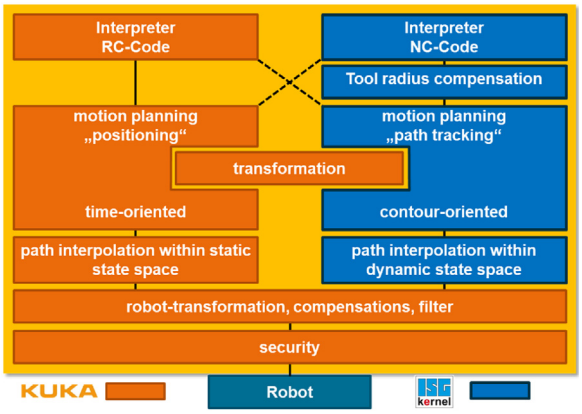

Fig. 33. Combination of RC and CNC functionalities in KUKA.CNC.

programming and minimize the need for retraining employees, leading to less reluctance using robots in the machining industry.

Practical examples prove that IRs can substitute machine tools, given their programming takes machining conditions into account. In an example from BAE Systems, two robots are used simultaneously for countersinking of predrilled holes on aircraft component production [120]. One robot performs machining, while the other assists the process by supporting (Fig. 34).

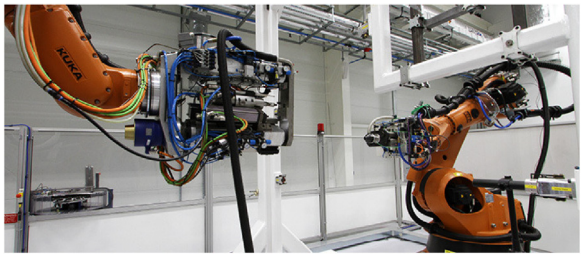

Fig. 34. Countersinking cell from BAE systems.

For machining very large workpieces, the working space of the robots may not be enough. For these cases, robots are moved around a part via automated guided vehicles (AGVs). Fig. 35(a) shows an application of milling a carbon fiber reinforced thermoplastic structure from the aerospace sector [121], whereas Fig. 35(b) presents polishing of a mold for a sailing boat [122].

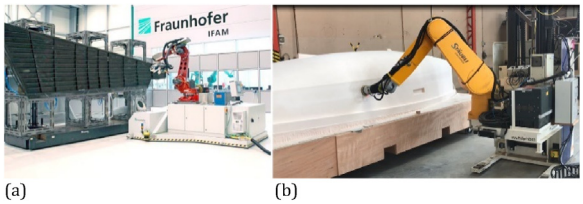

(a) (b)

Fig. 35. Mobile robots on AGVs: (a) aerospace [121]; (b) naval sector [122].

Fig. 36 shows how subscale machining on large aerospace parts is made possible by using an accuracy improved industrial robot mounted on an AGV [123]. Replacing machining centers for those kinds of applications requires highly accurate measurement systems and referencing strategies [72].

Although studies such as Klimchik et al. [62] showed that compensation algorithms can be applied to improve process quality, these were only validated in a laboratory environment and they have not yet been implemented in the industry. Hence, technology readiness levels of these solutions need to be more advanced for wider adoption of robotic machining in the high value manufacturing industry. Until then, industrial processes involving low cutting forces or low dimensional and surface quality requirements will remain suitable for industrial robots.

Please cite this article in press as: A. Verl, et al., Robots in machining, (2019), https://doi.org/10.1016/j.cirp.2019.05.009

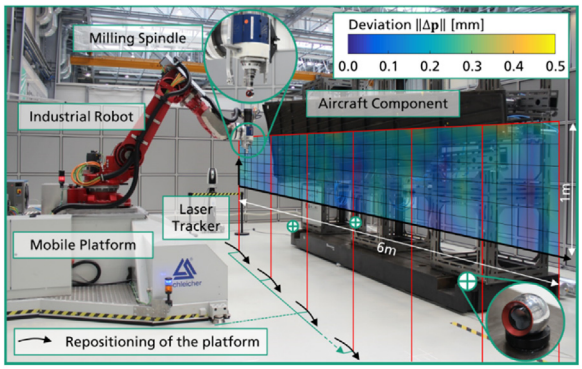

Fig. 36. Positioning accuracy in large workspaces [123].

4. Machining processes with industrial robots

In this section, we are offering a detailed overview of known machining processes that benefit from the deployment of industrial robots. We are also discussing methods of enabling robots for a wider range of machining applications based on current studies and research results.

4.1. Deburring

Deburring is a common manufacturing process which demands characteristics also common to robotic systems (e.g., flexibility or re-configurability, among others). Robots are still not widely used for performing this manufacturing task. Several advances have been made for improving the use of robots in deburring processes. The offline programming (OLP) allows simulating the process in virtual environments and automatically generating programs based on geometric approaches. For example, the use of OLP in conjunction with a touch probe-based strategy for robotic deburring of aerospace components [124]. Also, an offline simulation of finishing edges has been reported as beneficial for the automation of this process [125].

The problem of accurately localizing the workpiece is solved in industry mainly by using in-process measurement sensors that localize the workpiece for a subsequent accurate generation of the deburring path. For instance, the use of a vision assisted robotic system using 2D-images for automatic programming has been proposed in Ref. [126]. In industrial cases, workpiece inaccuracies are compensated under the allowed tolerance mainly due to the introduction of compliant tools that compensate surface irregularities while maintaining a defined force. Other compensation tools such as integrated pneumatic actuation systems have been proposed for tackling this limitation [127].

Numerous control laws and strategies have been proposed in order to compensate robot, process, and workpiece errors. The control methods can be categorized in two major approaches: impedance control and hybrid position/force control [128]. Examples of control applications are, for instance: the robot path generation method using hybrid force and visual servoing for reducing programming time [129]; tool-path modification based on direct teaching over the workpiece with a force control in normal/tangential direction [130]; the control strategy of mimicking human behavior during manual deburring [131].

Despite the previously introduced state of the art, remaining challenges have to be overcome in order to reduce the negative effects of the process and to facilitate the implementation of robotic deburring systems. These challenges are listed below:

- Robot, process, and product dependent tolerances make it difficult to reach the industry demanded accuracies.
- Robot cell cost efficiency may be limited due to complex settings and long programming times, especially given changeovers.
- Programming for robot deburring usually demands experts with further expertise in the process itself [132].
- Burr positions and dimensions are difficult to predict which makes the process highly variable.
- Additional sensors require specific parameterization, making the set-up of robot cells complex, especially given workpiece and process variations.
- The low stiffness of robot systems in comparison with CNC machines can cause difficulties for achieving high quality deburring, especially for iron and steel parts.
- The deburring of complex and large workpieces is difficult to achieve with robots due to the lack of absolute position accuracy.

Due to these challenges, manufacturing programming efforts and process quality requirements should be carefully investigated before applying robots in material removal. Robots still offer advantages: the machined part can be grasped and guided relative to the spindle, so that a fully automated work cycle is possible. Furthermore, large workspaces and high tool dexterity could be made available at a low cost.

4.1.1. Offline compensation of workpiece shape deviations

A fundamental problem affecting the process quality of deburring processes is that geometric shape deviations between the nominal CAD model and the manufactured parts may be beyond acceptable tolerances. To overcome this challenge, Kuss et al. [133] proposed an approach in which dimensional tolerance specifications of the manufactured part retrieved from the product design are then used to derive possible variations of the workpiece geometry model. The iterative closest point (ICP) algorithm is applied for identifying matching inaccuracies between CAD-generated and sensor-derived point clouds. These identified and modelled inaccuracies are later compensated in an OLP system to achieve better accuracies. Fig. 37 shows the experimental setup for the detection of workpiece shape deviations within a robotic deburring process. Deburring with shape deviations demonstrated a 57% decrease in the roundness standard deviation error, compared to deburring without shape deviation recognition.

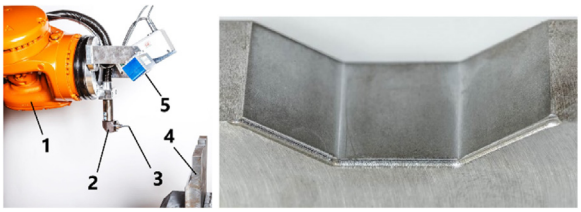

Fig. 37. Detecting workpiece shape deviations with a 3D sensor for robotic deburring processes (left). Test workpiece after the deburring process with detection of shape deviations (right) [133]. Key for the left image: 1. Industrial robot KUKA KR270; 2. Spindle Pferd PWS; 3. Milling tool; 4. Workpiece; 5. 3D sensor Ensenso N10.

4.1.2. Automatic OLP for sensor-based robotic deburring

In order to approach the complexity of programming robotic deburring systems, an automatic OLP for sensor-based robotic deburring has been proposed, facilitating the industrial implementation of these systems. Based on the Product, Process, and Robot (PPR) model, paths are generated which considers the constraints and DoF's of the robotic deburring process.

A laser scanner sensor is used for workpiece localization in the robot cell (Fig. 38). The ICP algorithm is later also used for compensating errors between the TCP and the edge to be deburred.

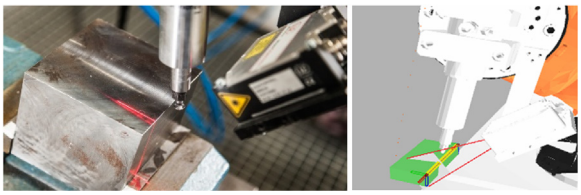

Fig. 38. Sensor-based robotic deburring (left), pre-programmed in an OLP environment (right) [134].

Output of this approach is an automatically generated program in which the expected measurements are also encoded and sent to the robot controller for later compensation [134]. Furthermore, the OLP system has been developed to embed sensor models for measurement optimization, considering sensor specifications and using sample-based planners and the intrinsic process DoF. Sensor and tool calibration algorithms have been proposed to provide satisfactory accuracies [134].

4.2. Incremental forming

In sheet metal forming, conventional processes are unable to meet the growing demand for shortening product development cycles due to their need for part dependent tools. Their time and cost intensive manufacturing prevent a reasonable usage in prototyping and small batch production [135,136]. The incremental sheet metal forming (ISF) process is able to overcome these challenges due to its high geometrical form flexibility and part independent tools, making it applicable for a wide range of industries [137–140].

In ISF, the final shape is produced by the incremental infeed of a hemispherical forming tool in the depth direction, and by its movement along the contour in the lateral direction on each level or on a helical path. This process called Roboforming (Fig. 39) can be executed by industrial robots, taking advantage of their high flexibility and distribution while losing the stiffness of the often-used modified CNC-machines [141]. A second supporting tool can be mounted on a second robot. It moves directly opposed to the forming tool and generates a predefined gap and force between the two hemispherical tools. This locally substitutes a die to improve the accuracy of the formed part [142]. Additional geometric elements need to be engineered in preparation of the Roboforming process chain after the target geometry CAD design of the sheet metal part is developed. These elements enable CAM-based path planning and the forming of the target geometry from a planar sheet metal.

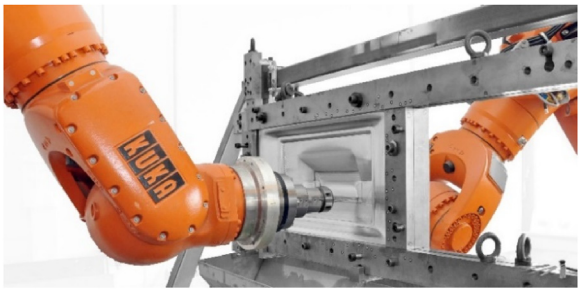

Fig. 39. Robot-based incremental sheet forming setup [143].

The applied CAM system determines the positions where the forming tool is in contact with the metal surface. A post processing step is required for robot program generation. All process parameters (e.g., contact force of the supporting tool) are defined in this step [144]. The forming of the extended geometry is executed by the incremental forming machinery. The sheet metal is then unclamped, annealed and cut down to the initial target geometry (Fig. 40).

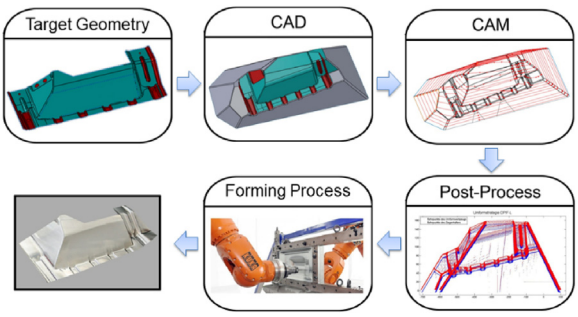

Fig. 40. Toolchain for robot-based incremental sheet forming [145].

During the execution of the forming process by the two cooperating industrial robots, the forces at the forming tool reach around 2000 N, using a typical deep-drawing steel with a sheet thickness of 1.0 mm. Those forces lead to a significant displacement of the forming tool's TCP and therefore a poor geometric accuracy of the produced part. Laurischkat [146] observed a displacement of the TCP of over 3 mm during the forming process using two KUKA KR360-1 (Fig. 41).

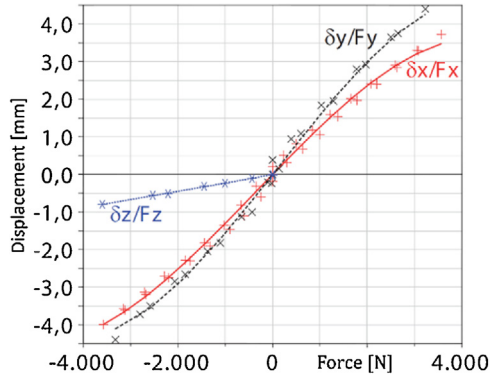

Fig. 41. Forming tool direct displacement, based on forming force [146].

To ensure a precise forming process, the displacement of the forming tool needs to be compensated. In literature there are various approaches to predict the resulting forming forces before the forming process [147,148]. However, those approaches lack the needed accuracy to enable a simulation-based compensation, especially for complex parts [82]. Therefore, an online-compensation of the robot position, based on the measured forming forces, is inevitable.

Abele et al. developed a flexible joint multibody dynamics system model for an industrial robot to describe its behavior based on the beforehand measured joint stiffnesses [149]. This model consists of a basic multibody system including the kinematic and kinetic parameters. The contained standard stiff joints are extended to flexible joints by the addition of joints in the direction of motion. Those are coupled to the driven joints by spring and damper elements. Analogously joints for tilting are added to describe the tilting behavior of the bearings. This elastic joint model is implemented into Matlab/Simulink via SimMechanics.

Laurischkat applied this flexible joint multibody system in Roboforming. The by a force torque sensor measured forming force is used to calculate the displacement of the TCP during the forming process. Afterwards, an inverse model is used to adjust the position via the robot sensor interface (RSI). Laurischkat [146] was able to improve the path accuracy significantly (Table 1) by using this approach. The online stiffness compensation is therefore a significant extension for the applicability of the process entailing an increase in geometric precision and increasing the formable sheet thickness making it indispensable in robot-based incremental sheet forming.

Table 1
Positioning accuracy in robot-based ISF [146].

Sheet thickness [mm]	Online compensation	Mean positioning error [mm]	Errors exceeding [%]	
			±0.3 mm	±0.6 mm
1.0	No	−0.98	83.6	70.0
	Yes	−0.04	2.9	0.0
1.5	No	−1.35	88.3	73.3
	Yes	−0.08	13.3	1.0

4.3. Grinding and polishing

Polishing of free form parts like turbine blades, dies and molds constitutes an important percentage of the total production time

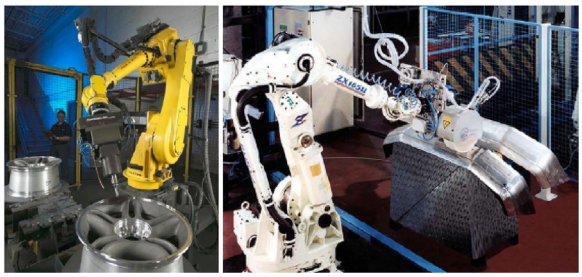

Fig. 42. Robotic polishing of: aluminum rim (left), car bumper (right) [151].

(17–29%) [150]. Various industrial parts require polishing as a last manufacturing step, as the examples in Fig. 42 show.

In polishing, the aim is to improve the surface finish rather than to alter part geometry or dimensions. Industrial robots are used in these operations as an alternative to machine tools. Considering the compliant tools used in polishing, the required motion accuracy from the articulated robot is not as high as for milling processes. As long as the robot can orient the end effector according to the part surface within the work space, it is very suitable to perform polishing processes. Literature shows studies on these processes where the major goal is to improve the efficiency and surface quality. The research has focused on end effector application, process analysis and path generation.

The design of end effector systems is of great importance in robotic polishing operations, especially for keeping a steady contact and consistent contact forces. Takeuchi et al. [152] used an air-actuated polishing end effector, where the contact force was adjusted by an interface of a linear roller slide and an air piston attached between the robot wrist and the tool. Mizugaki et al. [153] used loose abrasives in robotic polishing with a compliant end effector attached to a robot controller communicating with a CAD/CAM system. The efficiency of the system was demonstrated experimentally by preventing over-polishing at the edges.

In their work on automated process planning, Saito et al. [154] developed and implemented an expert system to plan the polishing of die and mold surfaces. Their system was able to suggest process plans for minimum cycle times, once performance requirements like surface quality and initial conditions were provided. The system was dependent on the knowledge of skilled mold polishers.

Tool path generation is a vital step towards an automated polishing process. Mizugaki et al. [155] proposed a novel method that used the planar Peano curve in the xy-plane and its orthogonal projection onto the free-form surface. They kept the end effector normal to the part surface considering the robot's working space. They concluded that this way, the polishing force can be controlled. In another study focusing on tool path generation, Tam et al. [156] succeeded in even tool path generation by addressing only time efficiency and surface quality issues. They showed that an accuracy of 0.01 mm can be achieved with robotic polishing of curved surfaces. Marquez et al. [157] offered a complete solution for robotic polishing of die-mold surfaces. They used the geometrical part definition obtained from the CAD model. The advantages of robotic automation for the manual polishing processes were clearly shown in terms of time and cost.

Tsai et al. [158] developed a robotic path planning system for the automated robotic polishing of molds. They utilized the IGES data format to create the geometric data structure. They then planned the tool path based on the intrinsic properties of the mold surface and process requirements. They demonstrated uniform coverage of the mold surface with satisfactory quality. In a study by Tsai et al. [159], a uniform material removal approach to improve automatic mold polishing is proposed. They obtained the mold surface geometry in the IGES format, which was re-generated in a NURBS surface model. They considered the intrinsic properties of the surface by considering the effective contact area along the polishing path for uniform material removal. The end effector velocity together with the polishing force were controlled in order to achieve uniform material removal. They obtained 60% improvement in profile error, and the material removal could be predicted accurately with an error margin lower than 6%.

For path control, Yang et al. [160] applied shape adaptive motion control with already integrated part measurement. They proposed a system containing four main blocks: surface measurement, surface reconstruction, tool trajectory planning, and axis motion control (Fig. 43). They implemented spatial spectral analysis in the first block, and proposed an optimal digitizing frequency. They then performed a spatial spectral B-spline method for surface reconstruction. In the third block, a motion profile was initially selected, then the tool locations were determined based on the reconstructed surface for improved accuracy. A software package was then developed and implemented in robotic polishing processes. They demonstrated benefits of the system for polishing the spherical surface of a doorstop.

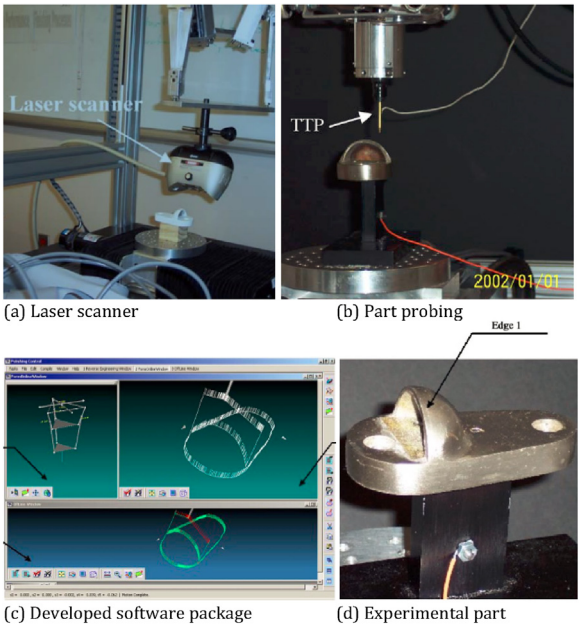

(a) Laser scanner (b) Part probing

(c) Developed software package (d) Experimental part

Fig. 43. Automated robotic polishing system [160].

Robotic grinding has also been used in manufacturing large scale hydro turbines by Alstom and Hydro-Quebec. They improved turbine efficiency by reducing surface roughness. In a related study of Sabourin et al. [161], the manual grinding process after the 5-axis milling of hydraulic turbines was robotized to obtain a better surface finish with less hydrodynamic friction, at a reduced total cost (Fig. 44). They improved grinding process parameters for a desired surface waviness and roughness, which was implemented on a full-scale Francis turbine blade. It was shown that the surface roughness can be lowered from Ra = 15 μm to Ra = 0.1 μm reaching a grinding rate of 5 h/m^2.

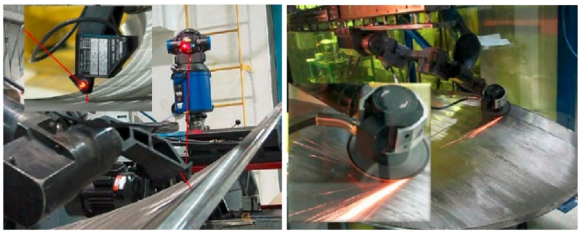

Fig. 44. Automated robotic polishing/grinding system for turbines [161]: Faro laser tracker used for proximity (left), polishing process (right).

In their work on automated robotic polishing systems, Ryuh et al. [162] integrated a six DoF articulated industrial robot with a pneumatic grinding tool controlled by a PC and a robot controller. They proposed a procedure to provide the path data to the robot. The data was automatically generated from the NC-data of a

previous machining process. This was a step forward towards automatic path planning for robotic polishing processes. They used an elastic material between the polishing pad and the holder, to further enhance the performance of the system in terms of the grinding contact.

In a recent study, Tian et al. [163] investigated solutions to improve cost and part quality in curved surface polishing. They established the physical relation between polishing force, robot, sensor and polishing tool. Then, they modelled the material removal distribution and combined this model with a suitable path spacing algorithm. They validated the system performance on NAK80 steel by showing that constant force control can be achieved by active and passive compliance force control.

4.4. Enabling industrial robots for specific tasks

The low eigenfrequencies and absolute positioning accuracies represent disadvantages of industrial robots in machining.

Measurements on a KUKA KR500-2 robot show that the first eigenfrequency is at 5.5 Hz. Its mode shape is a rotational deformation between the robot base frame and the rotating column. This low frequency comes from the poor stiffness in the gear box of the first joint [164]. During process planning, Denkena et al. consider the errors resulting from the gear boxes, such as compliance and backlash [69,165]. They use the results of the milling process simulation for a teach-less process monitoring. In the case of robot machining, effects like structural deviation and backlash are predicted based on the tool path and simulated cutting forces, and used for offline compensation. The backlash leads to a positioning error of 175–349 μm, which could be compensated by robot control. This compensation is still limited, because current machining state information like tool wear, clamping and thermal behavior are not regarded. To take process changes into account, Denkena et al. [164] present an approach for online compensation of deviations resulting from process forces. A model was investigated for calculating the pose-dependent stiffness for each pose. The machining robot is equipped with a force sensing spindle holder (Fig. 45) to measure process forces during the cutting operation and to increase process accuracy with an online compensation of the TCP deviation.

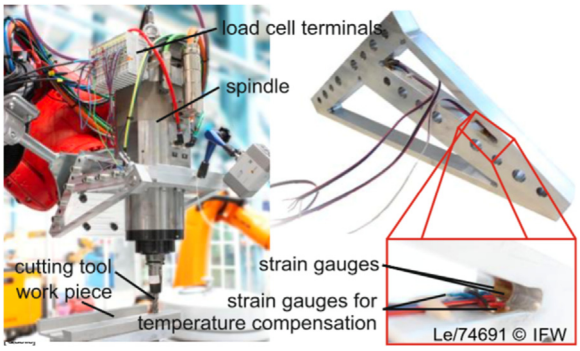

Fig. 45. Force sensing spindle holder for a KUKA KR 500-2 milling robot.

Milling tasks involve significantly higher load forces than handling and manipulating. This confronts robotic engineering with problems that have to be solved before industrial robots can compete with, or at least complement, conventional machine tools [112]. Due to their dynamic properties and relatively high compliance, serially linked robot arms are more susceptible to process forces than comparable machine tools [166]. This can lead to deflections from the commanded trajectory, and to strong natural oscillations. Fig. 46 illustrates the consequence of these two phenomena for a milling application.

The bend of the milled path in the upper part of Fig. 46 indicates that the end mill has been statically pushed away from its commanded trajectory. This deviation can be up to several millimeters, which is why Puzik et al. [167] refer to it as low

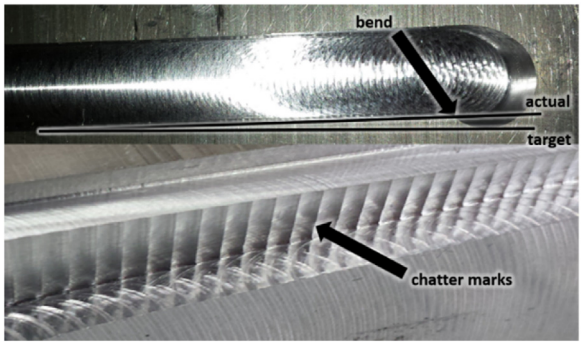

Fig. 46. Static deformation and dynamic instability when milling with robots [38].

trajectory accuracy. The lower part of Fig. 46 shows the result of dynamic instability: a sufficiently strong force excitation leads to a natural vibration of the end effector and therefore to waviness formation on the workpiece surface (chatter marks). Since the cutting force increases momentarily whenever the end mill cuts into one of these chatter marks, the robot structure is excited periodically with one of its eigenfrequencies. The vibrations caused by this self-excitement can become so strong that the machining process has to be stopped in order to avoid serious damage to the machine, the tool, or the workpiece [168]. Despite these qualitative shortcomings of milling robots compared to machine tools, their flexible applicability and their lower investment costs motivate a division of work: a milling robot processes a workpiece as much as possible, and then a machine tool performs the finishing. The latter can be used more efficiently and more profitably this way [112,169].

Several research studies aim to improve the accuracy, the vibration behavior and the achievable quality of milling results of industrial robots. To increase the kinematic stiffness and thereby the static stability, mechanical reinforcements are widespread. Machining robots with an increased degree of parallelism are already available on the market (e.g., ABB IRB 6660). Designing the spindle as a sixth axis and removing one axis and its compliance from the flux of forces is another constructional approach to the problem of static compliance-related errors [170]. These measures can improve the static and dynamic properties of robots, but reduce the usable workspace and the kinematic flexibility [84].

A common way to deal with instabilities and inaccuracies is the implementation of mathematical models for the offline simulation of different robot structure reactions. Kurze [171] proposed a model-based method to improve path accuracy and disturbance behavior. Since the model stiffness and damping parameters have been determined by analyzing free oscillations in only one pose, the results have been classified as not satisfactory by the author. Other works carried out experiments in various poses to determine the static compliances and use the measurement results to derive analytical models of the robot [118,172].

The common problem faced by model-based approaches is the dependency of static and dynamic properties on the robot's joint configuration [27,38,173]. Due to system complexity given by numerous joints and components, this interdependency is insufficiently described by a mathematical model [174]. Robot dynamics models are therefore either valid for just a small section of the workspace or insufficiently consider nonlinearities [175]. Recent studies attempt to identify the pose (end effector cartesian position and orientation) in an empirical dependency on process stability, with a high number of measurements conducted in different machining poses throughout the workspace. For this purpose, research groups carried out milling experiments in nine different poses in the xz-plane (y = 0 mm) of the workspace with feed in positive and negative x and y-direction, as seen in Fig. 47.

Milling wedges with linearly increasing cutting depth gives information about the correlation between depth of cut and processing stability. Oscillations of the robot structure are recorded with a force-sensing plate underneath the workpiece, and

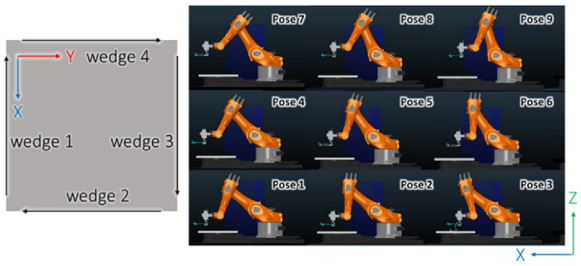

Fig. 47. Milling pattern (left) and machining poses [27].

acceleration sensors on the robot arm. The measurements lead to the following conclusions: (1) The robot has a strong dependency on the static and dynamic behavior of the machining pose and the feed direction. Further experimental investigations in this field are necessary. (2) An exclusive consideration of robot compliance values, as it has been assumed in many previous approaches, will be unsuccessful: for some machining poses, milling quality and process stability are higher, even though the robot structure is especially compliant for these joint configurations. Such approaches require a high amount of measurement and workload, but they yield promising results.

5. Trends in robotic machining

Having set the scope for deploying industrial robots in machining processes, we are now focusing in this chapter on other fields of applications for robots in machining.

5.1. Thin wall machining

Robotic assisted machining is particularly beneficial for thin wall parts, where problems such as high form errors and chatter are very common. Ozturk et al. [176] demonstrated the use of mobile rubber roller support that follows the feed motion of the machine tool. The rubber roller on the robot applies both support force and provides additional damping to the part. Hence, the maximum form error was decreased from 90 to 29 μm in a representative case (Fig. 48).

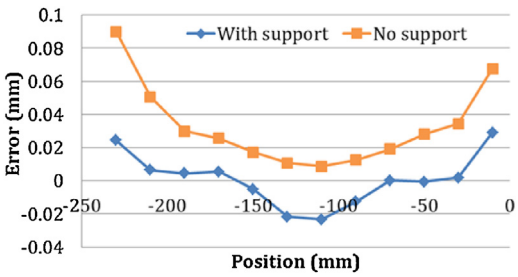

Fig. 48. Improvement in form error with the support.

Moreover, chatter problems experienced in the center of the part were eliminated, resulting in an improved surface quality (Fig. 49).

Support can be provided by different end effectors, such as rubber rollers and metal castors, which follow the feed motion of the machine tool. A dexterous hand can also be used as an additional support in order to increase the dynamic stiffness of the part (Fig. 50).

As both machine tool and robot are in motion during the process, there is a risk of collision between them. For this reason, the integration of the machine tool control and robot control needs to be established to achieve synchronous motion.

5.2. Dedicated kinematics

Machine tool productivity of industrial robots is still limited by the dynamic properties, as they influence the process stability.

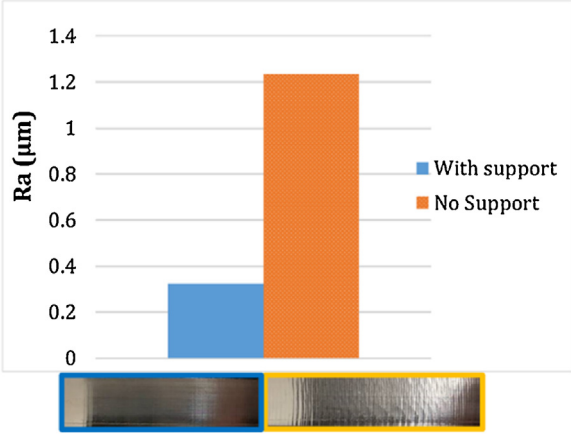

Fig. 49. Improvement in surface quality R_a with the support.

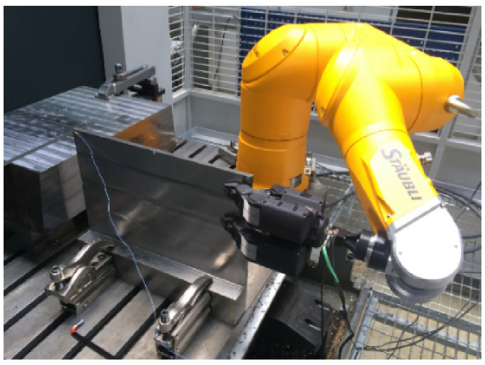

Fig. 50. Robotic hand support on a thin wall part.

These influences cannot be compensated with robot control because the ability to control the joint dynamics is limited by the cycle time of the robot control. One solution is the optimization of the whole robot kinematic chain and also of the drive concept. Denkena et al. [177] proposed an analytical comparison of three different machine kinematics (Fig. 51). The main objective was the development of a new cost-efficient machine tool for milling large aluminum and carbon fiber reinforced thermoplastic (CFRP) parts.

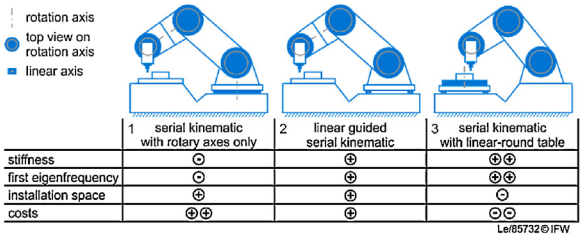

Fig. 51. Concepts and evaluation of machine tool kinematics [177].

The first concept is based on a serial kinematic. As the sixth joint is not required for five-sided machining, it is eliminated. For the second concept, a translational axis is used instead of the first rotational axis. This drives the whole robot kinematic chain, increasing the work space and decreasing the required length of the links. In the third concept, the linear axis actuates the workpiece table instead of the robotic arm kinematic chain. A rotational axis of the robotic kinematic chain is replaced by a rotary table. The replacement of the first rotational axis increases the stiffness by up to 35%, while the replacement of the guiding shoes on the next larger model has an insignificant influence. The third concept is the best solution for higher productivity, but is also more expensive. The second concept is useful when an inexpensive machine with optimized stiffness is required. Fig. 52 shows an analysis of the influence of machine components on the stiffness at the robot TCP.

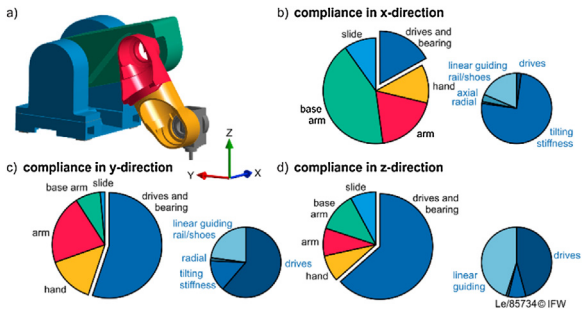

Fig. 52. Impact of the machine tool parts on the stiffness at TCP.

Due to the long-arm kinematic chain of industrial robots, joint stiffness has a big influence on the TCP position in machining applications. Measurements on a KUKA KR500-2 show that the stiffness at the TCP varies in a range of 0.5–1 N/μm depending on pose and force direction. The low joint stiffness is the reason for low eigenfrequencies in industrial robots. These vibrations reduce the surface quality in milling operations.

Denkena et al. developed a piezo-based, actuated robot arm to compensate for high dynamic vibrations of the TCP of an industrial robot [178]. Highly flexible piezo-based actuator foils and sensors were integrated into the robot structure. As CFRP is predestined for the integration of sensors, the robot arm was replaced by a CFRP component. The end effector can be positioned with sub-micrometer precision, enabling dynamic compensation of positioning errors. It can also be used to actively damp the structural vibration and to increase dynamic stiffness.

A further approach deals with the optimization of the drives. Industrial robot drives use gearboxes to achieve the high drive torques required to actuate the large mass of the serial structure. Denkena et al. [179] developed a new hybrid drive concept, which combines the advantage of a torque motor with the high torque of a servomotor with gearbox. In order to show the advantage of the new drive concept, it was tested in a two axes robotic kinematic chain. Each joint was equipped with a torque motor with a load-sided high-resolution encoder in addition to the conventional harmonic drive gearbox. The gear motor is used for axis positioning, as it can provide a high torque. The torque motor compensates for static and dynamic errors measured on the load-side. The hybrid drive concept increases the static joint stiffness in control ten times compared to the stiffness of an industrial robot.

5.3. Hybrid manufacturing

The most economic application of machining robots can be achieved when high flexibility or a large working space are needed. The combination of two or more process steps can be the basis of these applications. A hybrid manufacturing concept, combining additive and subtractive processes based on an industrial robot, represents an innovative approach to manufacturing technology.

Exemplary applications are changing the geometry of large molding dies for composite components [84] or body sheets, or the production of structural-components, especially for Ni-based alloys [117]. For the robot-based hybrid-manufacturing concept, different cladding techniques (e.g., friction surfacing) can be combined with a robotic milling process in order to produce near-net shape components for the finishing process (Figs. 53 and 54) [180].

Fig. 53. Robot-machining of laser-cladded paths [181].

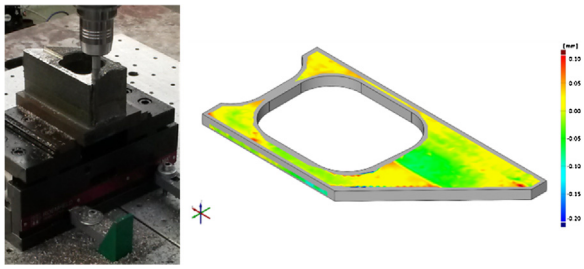

Fig. 54. Tolerances for machined Ni-alloys parts with industrial robots. (© PTW TU Darmstadt).

Other process combinations include drilling, reaming, assembly and quality assurance steps in one robot cell [182]. Supported by laser line scanning and qualified CAM tools, these processes are applied in one robot cell, thus enabling a hybrid manufacturing process in one clamping.

Skilled path planning in CAM-tools increases the accuracy – in terms of geometry and surface quality – due to lower tool deflections. Furthermore, the process combination and integration in one cell offers high resource savings. The hybrid production concept combined with robot compliance- and temperature compensation enables a high productivity and accuracy process for individual components made of difficult-to-machine alloys.

The large working space of robots can be used for the machining of structural lightweight parts — starting with medium sized parts like spring-strut domes for the automotive industry [103] up to very large components for aerospace or the shipbuilding industry.

The work space can be increased by adding a mobile self-driven platform carrying the machining robot [72]. Another field of application is the machining of large carbon composite and ceramic parts, due to the advantage of protecting the revolute joints of robots by excess pressure against superfine particles compared to sealed protections and bulky covers for linear machine ways and ball screws [183,16].

5.4. Reconfigurability

Modular robots are conceived as the composition of multiple blocks with uniform interfaces allowing for the transfer of mechanical forces and torque, electrical power, and communication through the robot. Building blocks consist of a primary structurally actuated unit and additional specialized units such as grippers, vision systems and energy storage units [184].

The adoption of modular and reconfigurable robots presents a number of advantages [184], such as versatility, robustness and lower costs over time. Examples of major results in the field of reconfigurable robotics can be found in Refs. [185–194]. More recent works deal with: (1) nesting mechanisms for robot modules [195–199]; (2) direct and inverse kinematics [200–203]; (3) communication and control [204–207]; (4) motion planning [208,209]; or (5) optimization of robot performance [210,211].

Since accuracy and reliability are more critical for a reconfigurable robot, the choice of the most appropriate structural configuration has an importance that goes beyond the mere satisfaction of workspace reach [212]. Also, their complexity demands further research efforts in the development of condition monitoring, fitting this kind of techniques to the peculiar needs and advantages of modular solutions [213–218].

In conclusion, the research on reconfigurable robotics for machining will face various open challenges: (i) developing flexible software frameworks for controlling flawlessly a wide, potentially unlimited range of kinematic chains; (ii) turning the concept of reconfigurability in a cost-effective, industrialized robust solution for manufacturing that can achieve out-of-the-box guaranteed, high-end performances.

5.5. Robot programming with function blocks

As of today, the three main available robot programming methods are: lead-through programming with a teach pendant, walk-through programming by guiding the robot at its end-effector, and offline programming with a CAM software.

A novel approach is function block programming. It bridges the gap between task planning systems and execution systems, and empowers robot controllers with intelligence. Whilst more common in human-robot-collaboration applications, it can also provide an additional advantage in robot machining. In function block programming, a non-linear task sequence plan can be mapped automatically to a set of function blocks, which can be readily dispatched to a chosen robot controller for task execution. The embedded algorithms of the function blocks are triggered inside the robot controller to accomplish the planned tasks. Feedback from human workers is processed and passed to the function blocks at the robot side for timely robot control.

A function blocks-based automation architecture differs from its classical counterparts as it enables adaptiveness at multiple levels. This ensures coping with high rates of component malfunctioning and handling complex system behavior and dynamics based on the co-ordination of a rich set of signals. Such adaptiveness, both architectural and behavioral, is driven by a need to accommodate external and internal changes, either deterministic or unpredictable. Each function block contains the control algorithms ruling the behavior of the resources at different levels in the automation system from a single control loop up to the supervision and planning levels. A robotics example can be seen in Fig. 55.

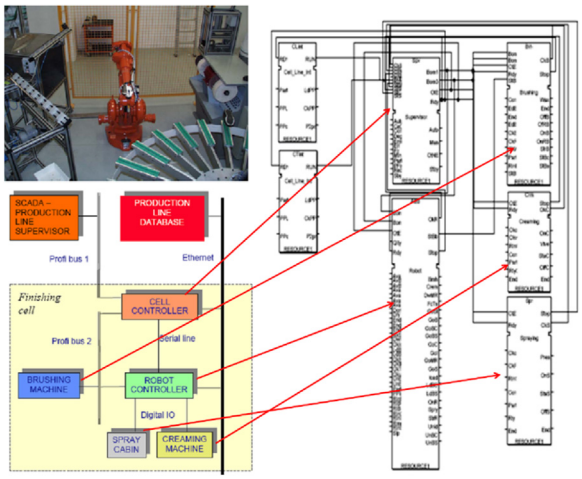

Fig. 55. Function block distributed control architecture of the robotic cell.

In robotic applications, examples of function blocks can be elementary functions such as "*move to*" or "*load tool_ID*", that can be implemented to populate a library of tasks, up to more complex functions addressing the process recipes and sequence of manufacturing tasks. These function blocks are then sequenced in a task schedule to execute specific machining processes such as the polishing example reported in Ref. [219].

5.6. AI in machines and collaborative robots

The new generation of industrial robots will need to embed highly advanced control systems, and be able to autonomously adapt to unexpected situations including performance degradation. This can be achieved by adapting the motion parameters. This typically limits their joint performance by reducing the most relevant factors (e.g., acceleration, speed, and deceleration). Path planning adaptation alternatively allows to reduce the movement of the degraded joints as much as possible by recomputing trajectories. Artificial intelligence (AI) techniques such as machine learning and reinforcement learning frameworks can be developed to allow task experts without AI or programming expertise to teach the robots their initial task and then support their continuous learning over the robot's deployment. The goal is to enable autonomous robots to learn a large repertoire of behavioral skills with minimal human intervention. However, robotic AI applications often compromise the autonomy of the learning process in favor of achieving training times. This typically involves introducing hand-engineered logic representations and human demonstrations. In robotic learning, research work has explored model-based and model-free learning algorithms.

Model-based algorithms include a variety of dynamics estimation schemes [220] such as Gaussian processes, mixture models, and local linear system estimation. Deep neural network policies have been combined with model-based learning in the context of guided policy search algorithms [221,222]. Such approaches are exploited for example for scenarios demanding close coordination between vision and control (developing policies that map raw image observations directly to torques at the robot's motors), or in general in situations where it is necessary to learn complex feedback control policies mapping high-dimensional sensory inputs to motor torques.

Model-free algorithms include policy search [223] and function approximation methods [224] that have recently been combined with deep neural networks for learning complex tasks [225]. Direct policy gradient methods offer the benefit of unbiased gradient estimates, but tend to require more experience, since on-policy estimators preclude reuse of past data.

In manufacturing, machine learning can serve an additional role in design and optimization of processes [226–229], but demands future research on real-time processing and control. In current applications, the robot motion strategy and machining parameters are adapted in real time based on a sensing system supporting in-process data collection, their fusion and interpretation. The optimization logics rely on specific reference quality KPIs. Any anomalous behavior corresponding to the violation of the quality indicators results in triggering the optimization model and enabling the process adaptation logic. The optimization model can be designed based on various techniques, including AI. Future works will also consider non-time-critical functions and particularly additional awareness and computational power [230].

6. Conclusions

An increasing role of robots in manufacturing is noticeable, especially in machining, as exemplified throughout this paper. We have outlined and investigated opportunities of exploiting the advantages of robots in this area. One of the trends in robotic manufacturing is the implementation of accurate and easy-to-use intuitive programmable systems. The approaches presented in chapter 4 are examples of such systems. Based on this trend and the remaining challenges, future directions in this field could be:

- Simulation of robotic systems could be interfaced with analytical or numerical models to compute robot motion adaptations for increased tool path accuracy.
- Accessible implementation of robot systems with intrinsic sensors (i.e. force/torque or vision) capable of automatically adapting motions in respect to the machining task, thus enabling improved process control.
- The path planning process could be optimized using process redundancy for improving the process quality.
- After automatically checking product quality, machine learning algorithms for process optimization could be offered in a cloud-service platform.
- Development of input devices for facilitating the programming experience. Such devices could record process characteristics and update these in robot systems. Furthermore, robot systems could learn and be trained by mimicking professional workers.

This paper addresses these challenges and shows how they can be overcome for a wider implementation of robots in machining.

After a theoretical insight, we have presented the possibilities of identifying and determining system parameters. Different approaches for overcoming inherent shortcomings of robots in machining are distinguishable. The limited static and dynamic stiffness of robot joints and links still results in insufficient rigidity of the TCP, in turn impacting machining accuracy. We have also shown that the static Cartesian stiffness of industrial robots is up to 50 times lower than the corresponding stiffness of a typical CNC machine tool. However, manufacturing inaccuracies in robot production can be compensated by various methods.

Due to system complexity, state of the art offline compensation is always a simplification and approximation of the real situation. On the other hand, online compensation can use sensor data from the real setting, while system complexity hinders the deployment of complex algorithms. Numerous solutions are available, but always for special purposes (i.e. increasing stiffness but not accuracy; or increasing accuracy due to control problems, but not due to process forces). These solutions still require specialist knowledge and are not yet applicable in the industry.

However, not only their lower cost offers robot applications an advantage in machining tasks. Several efforts towards improving machining robot accuracy could be identified with promising results. Studies show that only a small fraction of all industrial robots deployed worldwide in recent years were intended for machining tasks, a small number compared to their potential in this area. In order to deploy robots to directly perform manufacturing tasks like machining, further investigations are necessary. Current trends show efforts being made towards developing dedicated kinematics, new drive concepts and new fields of application. The collected findings presented here can offer support in this direction.

Acknowledgements

Contributions to this keynote paper from the following colleagues are gratefully acknowledged: Ali Karim, Michael Neubauer, Mihai Drăgan, Eberhard Abele, Berend Denkena, Bernd Kuhlenkötter, Thomas Bauernhansl, Martin Hägele, Eckart Uhlmann, Wolfgang Hintze, Klas Nilsson, Hendrik Van Brussel, Christian Baier, Felix Hähn, Lars Lienenlüke, Lukas Gründel, Thomas Lepper, Benjamin Bergmann, and Dirk Niermann.

References

[1] IFR Statistical Department (2018) *World Robotics 2018 Industrial Robots*.
[2] https://ifr.org/ifr-press-releases/news/robots-double-worldwide-by-2020. Retreived 21 September 2018.
[3] Corke P (2011) Robotics, Vision and Control: Fundamental Algorithms in MATLAB. *Volume 73 of Springer Tracts in Advanced Robotics*, Springer Science & Business Media.
[4] Altintas Y (2012) *Manufacturing Automation: Metal Cutting Mechanics, Machine Tool Vibrations, and CNC Design*, 2nd edn. Cambridge U. Press.
[5] Appleton E, Williams DJ (1987) *Machining with Robots, in Industrial Robot Applications*, Dordrecht, Springer Netherlands. p. 170.
[6] Devol Jr. GC, "Programmed Article Transfer" U.S. Patent 2988237, issued Jun. 31, 1961.
[7] International Organization for Standardization (ISO) (2012) *Robots and Robotic Devices: Vocabulary*, 2nd edn. . 25.040.30, 01.040.25, 2012(ISO 8373:). https://www.iso.org/standard/55890.html. Accessed 7 August 2018.
[8] Spong MW, Hutchinson S, Vidyasagar M (2006) *Robot Modeling and Control*, Wiley, Hoboken, NJ op.
[9] Murray RM, Li Z, Sastry SS (1994) *A Mathematical Introduction to Robotic Manipulation*, CRC Press, Boca Raton, Fla.
[10] Jubien A, Gautier M, Janot A (2014) Dynamic Identification of the Kuka LWR Robot Using Motor Torques and Joint Torque Sensors Data. *IFAC Proceedings* 47(3):8391–8396.
[11] Janot A, Vandanjon PO, Gautier M (2014) A Generic Instrumental Variable Approach for Industrial Robot Identification. *IEEE Transactions on Control Systems Technology* 22(1):132–145.
[12] Gautier M, Janor A, Vandanjon PO (2008) DIDIM. A New Method for the Dynamic Identification of Robots from Only Torque Data. *2008 IEEE International Conference on Robotics and Automation (ICRA)* 2122–2127.
[13] Wu J, Wang J, You Z (2010) An Overview of Dynamic Parameter Identification of Robots. *Robotics and Computer-Integrated Manufacturing* 26(5):414–419.
[14] Hartenberg RS, Denavit J (1965) Kinematic Synthesis of Linkages. *McGraw-Hill Series in Mechanical Engineering*, McGraw-Hill, New Yorkp. 435.
[15] Lipkin H (2005) A Note on Denavit–Hartenberg Notation in Robotics. *Volume 7: 29th Mechanisms and Robotics Conference Parts A and B* 921–926. http://dx.doi.org/10.1115/DETC2005-85460. ISBN 0-7918-4744-6.
[16] Siciliano B, Khatib O, (Eds.) (2016), *Springer Handbook of Robotics*, Springer.
[17] Bongardt B (2013) Sheth–Uicker Convention Revisited. *Mechanism and Machine Theory* 69:200–229. ISSN 0094-114X.
[18] Pan Z, Zhang H, Zhu Z, Wang J (2006) Chatter Analysis of Robotic Machining Process. *Journal of Materials Processing Technology* 173:301–309.
[19] Abele E, Weigold M, Rothenbücher S (2007) Modeling and Identification of Industrial. Robot for Machining Applications. *CIRP Annals Manufacturing Technology* 56(1):387–390.
[20] Bondarenko D, Pashkevich A, Briot S, Ritou M, Furet B (2012) Elasto-Dynamic Model of Robotic Milling Process Considering Interaction between Tool and Workpiece. *Proceedings of ASME 2012 11th Biennial Conference on Engineering Systems Design and Analysis* 1–10.
[21] Cen L, Melkote SN (2017) Effect of Robot Dynamics on the Machining Forces in Robotic Milling. *Procedia Manufacturing* 10:486–496.
[22] Cordes M, Hintze W, Altintas Y (2019) Chatter Stability in Robotic Milling. *Robotics and Computer-Integrated Manufacturing* 55(A):11–18. ISSN 0736-5845.
[23] Cen L, Melkote SN, Castle J, Appelman H (2018) A Method for Mode Coupling Chatter Detection and Suppression in Robotic Milling. *Journal of Manufacturing Science and Engineering* 140. 081015-1.
[24] Mousavi S, Gagnol V, Bouzgarrou BC, Ray P (2017) Dynamic Modeling and Stability Prediction in Robotic Machining. *The International Journal of Advanced Manufacturing Technology* 88:3053–3065.
[25] Tunc LT, Stoddart D (2017) Tool Path Pattern and Feed Direction Selection in Robotic Milling for Increased Chatter-Free Material Removal Rate. *The International Journal of Advanced Manufacturing Technology* 89:2907–2918.
[26] Karim A, Corcione E, Jäger J, Verl A (2018) Experimental Determination of Compliance Values for a Machining Robot. *IEEE/ASME International Conference on Advanced Mechatronics (AIM)*, .
[27] Karim A, Schmid S, Verl A (2017) Pose and Feed-Direction Dependency Analysis for Milling Tasks With Industrial Robots. *24th International Conference on Production Research (ICPR)*, .
[28] Dumas C, Caro S, Cherif M, Garnier S, et al (2012) Joint Stiffness Identification of Industrial Serial Robots. *Robotica* 30:649.
[29] http://cognibotics.com/technology/dynamic-modeling/. Retreived 25 September 2018.
[30] Nilsson K. Method and System for Determination of at Least One Property of a Joint, Patent No. BR112015008933 (2), issued Jul. 4 2017.
[31] Nilsson K, Nilsson A. Method and System For Determination of at Least One Property of a Manipulator, Patent No. ES2644939 (T3), issued Dec. 1 2017.
[32] Lehmann C, Olofsson B, Nilsson K, Halbauer M, Haage M, Robertsson A, Sörnmo O, Berger U (2013) Robot Joint Modeling and Parameter Identification Using the Clamping Method. *7th IFAC Conf on Manuf Modelling, Management, and Control*, 813–818.
[33] Celikag H, Sims ND, Ozturk E. Cartesian, Stiffness Optimization for Serial Arm Robots, Proc CIRP, 8th CIRP Conf. on High Perf. Cutting (HPC 2018).
[34] Cen L, Melkote SN (2017) CCT-Based Mode Coupling Chatter Avoidance in Robotic Milling. *Journal of Manufacturing Processes* 29:50–61.
[35] Chen S-F, Kao I (2000) Conservative Congruence Transformation for Joint and Cartesian Stiffness Matrices of Robotic Hands and Fingers. *The International Journal of Robotics Research* 19(9):835–847.
[36] Lienenlüke L, Gründel L, Storms S, Brecher C (2018) Model-Based Process Planning for Milling Operations Using Industrial Robots. *3rd Conference on Control and Robotics Engineering (ICCRE)*, .
[37] Mejri S, Gagnol V, Le T-P, Sabourin L, Ray P, Paultre P (2016) Dynamic Characterization of Machining Robot and Stability Analysis. *The International Journal of Advanced Manufacturing Technology* 82:351–359.
[38] Karim A, Hitzer J, Lechler A, Verl A (2017) Analysis of the Dynamic Behaviour of a Six-Axis Industrial Robot within the Entire Workspace in Respect of Machining Tasks. *2017 IEEE International Conference on Advanced Intelligent Mechatronics (AIM)*, .
[39] Kim J, Kim SR, Kim SJ, Kim DH (2010) A Practical Approach for Minimum-Time Trajectory Planning for Industrial Robots. *Industrial Robot: An International Journal* 37(1):51–61.
[40] Constantinescu D, Croft EA (2000) Smooth and Time-Optimal Trajectory Planning for Industrial Manipulators Along Specified Paths. *Journal of Robotic Systems* 17(5):233–249.
[41] Piazzi A, Visioli A (2000) Global Minimum-Jerk Trajectory Planning of Robot Manipulators. *IEEE Transactions on Industrial Electronics (1982)* 47(no. 1):140–149.
[42] Gasparetto A, Lanzutti A, Vidoni R, Zanotto V (2012) Experimental Validation and Comparative Analysis of Optimal Time-Jerk Algorithms for Trajectory Planning. *Robotics and Computer-integrated Manufacturing* 28(2):164–181.
[43] Gasparetto A, Zanotto V (2007) A New Method for Smooth Trajectory Planning of Robot Manipulators. *Mechanism and Machine Theory* 42(4):455–471.
[44] Huang P, Chen K, Yuan J, Xu Y (2007) Motion Trajectory Planning of Space Manipulator for Joint Jerk Minimization. *Proc. 2007 IEEE Int. Conf. Mechatronics Autom. ICMA 2007*, 3543–3548.
[45] Zha XF (2002) Optimal Pose Trajectory Planning for Robot Manipulators. *Mechanism and Machine Theory* 37(10):1063–1086.
[46] Perumaal S, Jawahar N (2012) Synchronized Trigonometric S-Curve Trajectory for Jerk-Bounded Time-Optimal Pick and Place Operation. *International Journal of Robotics and Automation* 27(4).
[47] Macfarlane S, Croft EA (2003) Jerk-Bounded Manipulator Trajectory Planning: Design For Real-Time Applications. *IEEE Transactions on Robotics and Automation* 19(1):42–52.

[48] Nguyen KD, Ng TC, Chen IM (2008) On Algorithms for Planning S-Curve Motion Profiles. *International Journal of Advanced Robotic Systems* 5 (1):99–106.
[49] Porawagama CD, Munasinghe SR (2014) Reduced Jerk Joint Space Trajectory Planning Method Using 5-3-5 Spline for Robot Manipulators. *7th International Conference on Information and Automation for Sustainability*, 1–6.
[50] Rossi C, Savino S (2013) Robot Trajectory Planning by Assigning Positions and Tangential Velocities. *Robotics and Computer-Integrated Manufacturing* 29 (1):139–156.
[51] Avram O, Valente A (2016) Trajectory Planning for Reconfigurable Industrial Robots Designed to Operate in a High Precision Manufacturing Industry. *49th CIRP Conference on Manufacturing Systems (CIRP-CMS 2016)*, .
[52] Valente A, Baraldo S, Carpanzano E (2017) Smooth Trajectory Generation for Industrial Robots Performing High Precision Assembly Processes. *CIRP Annals Manufacturing Technology* 66(1):17–20.
[53] Baraldo S, Valente A (2017) Smooth Joint Motion Planning for High Precision Reconfigurable Robot Manipulators. *2017 IEEE International Conference on Robotics and Automation (ICRA)*, 845–850.
[54] Saboori A, et al (2018) The Capacity of Cold Spray Additive Manufacturing Technology for Metallic Part Repairing. *Euro PM2018*, . Submitted.
[55] Mekaouche A, Chapelle F, Balandraud X (2015) FEM-Based Generation of Stiffness Maps. *IEEE Transactions on Robotics* 31(1):217–222.
[56] Nof SY, (Ed.) (1999), *Handbook of Industrial Robotics*. 2nd ed. ISBN: 978-0-471-17783-8.
[57] Asada H, Slotine JJE (1992) *Robot Analysis and Control*, John Wiley & Sons, Inc., New York, NY, USA. ISBN:0471830291.
[58] Bi S, Liang J (2011) Robotic Drilling System for Titanium Structures. *The International Journal of Advanced Manufacturing Technology* 54(May (5–8)):767–774.
[59] Zhan Q, Wang X (2012) Hand–Eye Calibration and Positioning for a Robot Drilling System. *The International Journal of Advanced Manufacturing Technology* 61(July(5–8)):691–701.
[60] Garniera S, Subrina K, Waiyaganb K (2017) Modelling of Robotic Drilling. *Procedia CIRP* 58:416–421.
[61] Klimchik A, Wu Y, Caro S, Furet B, Pashkevich A (2014) Accuracy Improvement of Robot-Based Milling Using an Enhanced Manipulator Model. *Advances on Theory and Practice of Robots and Manipulators Mechanisms and Machine Science*, vol. 22. 73–81.
[62] Klimchik A, Bondarenko D, Paskkevich A, Briot S, Furet B, et al (2014) Compliance Error Compensation in Robotic-Based Milling. Ferrier JL, (Ed.) *Informatics in Control Automation and Robotics*, Lecture Notes in Electrical Engineering 283. 197–214.
[63] Altintas Y (2000) *Manufacturing Automation*, Cambridge University Press.
[64] Schneider U, Drust M, Ansaloni M, Lehmann C, Pellicciari M, Leali F, Gunnink JW, Verl A (2016) Improving Robotic Machining Accuracy through Experimental Error Investigation and Modular Compensation. *The International Journal of Advanced Manufacturing Technology* 85:3–15.
[65] Schneider U, Ansaloni M, Drust M, Leali F, Verl A (2013) Experimental Investigation of Sources of Error in Robot Machining. Neto P, Moreira AP, (Eds.) *Robotics in Smart Manufacturing*, Communications in Computer and Information Science 371. 14–26.
[66] Diaz Posada JR, Schneider U, Sridhar A, Verl A (2017) Automatic Motion Generation for Robotic Milling Optimizing Stiffness with Sample-Based Planning. *Machines* 5(3):1–26. http://dx.doi.org/10.3390/machines5010003.
[67] Slavkovic NR, Milutinovic DS, Glavonjic MM (2014) A Method for Off-Line Compensation of Cutting Force-Induced Errors in Robotic Machining by Tool Path Modification. *The International Journal of Advanced Manufacturing Technology* 70:2083–2096.
[68] Tyapin I, Kaldestad KB, Hovland G (2015) Off-Line Path Correction of Robotic Face Milling Using Static Tool Force and Robot Stiffness. *IEEE/RSJ International Conference on Intelligent Robots and Systems* 5506–5511.
[69] Brüning J, Denkena B, Dittrich MA, Park HS (2016) Simulation Based Planning of Machining Processes with Industrial Robots. *Procedia Manufacturing* 6:17–24.
[70] Cordes M, Hintze W (2017) Offline Simulation of Path Deviation due to Joint Compliance and Hysteresis For Robot Machining. *The International Journal of Advanced Manufacturing Technology* 90:1075–1083.
[71] Hollerbach JM, Suh KI-C (1987) Redundancy Resolution of Manipulators through Torque Optimization. *IEEE Robotics & Automation Magazine* RA-3 (4):308–316.
[72] Susemihl H, Brillinger C, Stürmer SP, Hansen S, Boehlmann C, Kothe S (2017) Referencing Strategies for High Accuracy Machining of Large Aircraft Components with Mobile Robotic Systems. *SAE Technical Paper 2017-01-2166*. http://dx.doi.org/10.4271/2017-01-2166.
[73] Andres J, Gracia L, Tornero J (2011) Calibration and Control of a Redundant Robotic Workcell For Milling Tasks. *International Journal of Computer Integrated Manufacturing* 24(6):561–573.
[74] Xiao W, Huan J (2012) Redundancy and Optimization of a 6R Robot for Five-Axis Milling Applications: Singularity, Joint Limits and Collision. *Production Engineering Research and Development* 6:287–296.
[75] Sabourin L, Subrin K, Cousturier R, Gogu G, Mezouar Y (2016) Redundancy-Based Optimization Approach to Optimize Robotic Cell Behaviour: Application to Robotic Machining. *Industrial Robot: An International Journal* 42 (2):156–166.
[76] Mousavi S, Gagnol V, Bouzgarrou B, Ray P (2017) Control of a Multi Degrees Functional Redundancies Robotic Cell for Optimization of the Machining Stability. *Procedia CIRP* 58:269–274.
[77] Tobias SA (1965) *Machine-Tool Vibration*, Blackie & Son Ltd., London.
[78] Yuan L (2017) *A Study of Chatter in Robotic Machining and A Semi-Active Chatter Suppression Method Using Magnetorheological Elastomers (MREs). M. Eng. Thesis*, School of Mechanical, Material, Mechatronic and Biomedical Engineering, University of Wollongong, Australia.
[79] Alici G, Shirinzadeh B (2005) Enhanced Stiffness Modeling, Identification, and Characterization For Robot Manipulators. *IEEE Transactions on Robotics* 21 (4):554–564.
[80] Dumas C, Caro S, Garnier S, Furet B (2011) Joint Stiffness Identification of Six-Revolute Industrial Serial Robots. *Robotics and Computer-Integrated Manufacturing* 27:881–888.
[81] Lo CC, Hsiao CY (1998) A Method of Tool Path Compensation For Repeated Machining Process. *International Journal of Machine Tools and Manufacture* 38 (3):205–213.
[82] Belchior J, Guillo M, Courteille E, Maurine P, Leotoing L, Guines D (2013) Off-Line Compensation of the Tool Path Deviations on Robotic Machining: Application to Incremental Sheet Forming. *Robotics and Computer-integrated Manufacturing* 29(4):58–69.
[83] Barnfather JD, Goodfellow MJ, Abram T (2016) Development and Testing of an Error Compensation Algorithm For Photogrammetry Assisted Robotic Machining. *Measurement* 94:561–577.
[84] Zäh MF, Rösch O (2014) Improvement of the Machining Accuracy of Milling Robots. *Production Engineering* 8(6):737–744.
[85] Tunc LT, Shaw J (2016) Experimental Study on Investigation of Dynamics of Hexapod Robot For Mobile Machining. *The International Journal of Advanced Manufacturing Technology* 84(5-8):817–830.
[86] Tunc LT, Shaw J (2016) Investigation of the Effects of Stewart Platform-Type Industrial Robot On Stability Of Robotic Milling. *The International Journal of Advanced Manufacturing Technology* 87(1-4):189–199.
[87] Zhang H, Wang J, Zhang G, Gan Z, Pan Z, Cui H, Zhu Z (2005) Machining With Flexible Manipulator: Toward Improving Robotic Machining Performance. *IEEE/ASME (AIM) International Conference on Advanced Intelligent Mechatronics*, 1127–1132.
[88] Shi X, Zhang F, Qu X, Liu B (2016) An Online Real-Time Path Compensation System for Industrial Robots Based on Laser Tracker. *International Journal of Advanced Robotic Systems* 13(5). 1729881416663366.
[89] Zaghbani I, Songmene V, Bonev I (2013) An Experimental Study on the Vibration Response of a Robotic Machining System. *Proceedings of the Institution of Mechanical Engineers Part B: Journal of Engineering Manufacture* 227(6):866–880.
[90] Maurotto A, Tunc LT (2017) Effects of Chattering on Surface Integrity in Robotic Milling of Alloy 690. *Pressure Vessels and Piping Conference ASME 2017*. pp. V06AT06A004, 6 pages.
[91] Blomdell A, Bolmsjö G, Cederberg P, Isaksson M, Johansson R, Haage M, Nilsson K, Olsson M, Olsson T, Robertsson A, Wang J (2005) Extending an Industrial Robot Controller. *IEEE Robotics & Automation Magazine* 85–94.
[92] Bottero A, Gerio G, Perna V, Gagliano A (2014) Adaptive Control Techniques and Feed Forward Compensation of Periodic Disturbances in Industrial Manipulators. *IEEE/ASME 10th International Conference on Mechatronic and Embedded Systems and Applications (MESA)* 1–7.
[93] KUKA Robot Sensor Interface 3.2, KUKA Roboter GmbH.
[94] Olsson T, Haage M, Kihlman H, Johansson R, Nilsson K, Robertsson A, Björkman M, Isaksson R, Ossbahr G, Brogårdh T (2010) Cost-Efficient Drilling Using Industrial Robots with High-Bandwidth Force Feedback. *Robotics and Computer-integrated Manufacturing* 26:24–38.
[95] Pan Z, Zhang H (2008) Robotic Machining from Programming to Process Control: A Complete Solution By Force Control. *Industrial Robot an International Journal* 35(5):400–409.
[96] Schneider U, Diaz Posada JR, Drust M, Verl A (2013) Position Control of an Industrial Robot Using an Optical Measurement System for Machining Purposes. *Proceedings of the 11th International Conference on Manufacturing Research (ICMR2013)* 307–312.
[97] Schneider U, Olofsson B, Drust M, Robertsson A, Hägele M, Johansson R (2014) Integrated Approach to Robotic Machining With Macro/Micro-Actuation. *Robotics and Computer-integrated Manufacturing* 30:636–647.
[98] Diaz Posada JR, Schneider U, Pidan S, Geravand M, Stelzer P, Verl A (2016) High Accurate Robotic Drilling With External Sensor and Compliance Model-Based Compensation. *Proceedings of the IEEE International Conference on Robotics and Automation (ICRA)* 3901–3907.
[99] Moeller C, Schmidt HC, Koch P, Boehlmann C, Kothe S, Wollnack J, Hintze W (2017) Real Time Pose Control of an Industrial Robotic System for Machining of Large Scale Components in Aerospace Industry Using Laser Tracker System. *SAE International Journal of Aerospace* 10(2).
[100] Cen L, Melkote SN (2017) A Wireless Force-Sensing and Model-Based Approach for Enhancement of Machining Accuracy in Robotic Milling. *IEEE/ASME Transactions on Mechatronics* 21(5):2227–2235.
[101] Bongardt T (2004) *Methode zur Kompensation betriebsabhängiger Einflüsse auf die Absolutgenauigkeit von Industrierobotern, Dissert*, TU München, Utz.
[102] Abele E, Polle W, Ehm A, Troure M (2013) Spanende Bearbeitung mit industrierobotern - thermische einflüsse auf die bearbeitungsgenauigkeit. *Werkstattstechnik*. online, no. 9.
[103] Ehm A (2016) Einsatz von Industrierobotern für die Bohrbearbeitung an automobilen Strukturbauteilen unter Berücksichtigung des thermischen Verlagerungsverhaltens und der Prozessinteraktion, Schriftreihe des PTW "Innovation Fertigungstechnik". *Darmstadt*.
[104] Reinhart G, Gräser R-G, Klingel R (1998) Qualification of Standard Industrial Robots to Cope With Sophisticated Assembly Tasks. *CIRP Annals Manufacturing Technology* 47(1). http://dx.doi.org/10.1016/S0007-8506(07)62772-3.
[105] Du G, Zhang P (2013) Online Robot Calibration Based on Vision Measurement. *Robotics and Computer-Integrated Manufacturing* 29(6). http://dx.doi.org/10.1016/j.rcim.2013.05.003.
[106] Wiest U (2009) *Kinematische Kalibrierung von Industrierobotern. Dissertation*, Universität Karlsruhe, Karlsruhe.
[107] Boochs F, Schutze R, Simon C, Marzani F, Wirth H, Meier J (2010) Increasing the Accuracy of Untaught Robot Positions by Means of a Multi-Camera System. *International Conference on Indoor Positioning and Indoor Navigation (IPIN)*.

[108] Santolaria J, Conte J, Ginés M (2013) Laser Tracker-Based Kinematic Parameter Calibration of Industrial Robots by Improved CPA Method and Active Retroreflector. *The International Journal of Advanced Manufacturing Technology* 66(9):2087–2106.
[109] Yin S, et al (2014) Real-time Thermal Error Compensation Method for Robotic Visual Inspection System. *The International Journal of Advanced Manufacturing Technology* 75(5-8):933–946.
[110] Elbestawi MA, Bone GM, Tern PW (1992) An Automated Planning, Control, and Inspection System For Robotic Deburring. *CIRP Annals Manufacturing Technology* 397. Manuf Tech.
[111] Möller C, Schmidt H, et al (2016) Enhanced Absolute Accuracy of an Industrial Milling Robot Using Stereo Camera System. *Procedia Technology* 389–398. http://dx.doi.org/10.1016/j.protcy.2016.08.050.
[112] Karim A, Verl A (2013) Challenges and Obstacles in Robot-Machining. *44th IEEE International Symposium on Robotics (ISR)* 224–228.
[113] Bongardt T (2003) *Methode Zur Kompensation Betriebsabhängiger Einflüsse Auf Die Absolutgenauigkeit Von Industrierobotern. Dissertation*, TU München.
[114] Gossel O (1996) *Steigerung der Genauigkeit von Industrierobotern basierend auf einer durchgängigen Genauigkeitsanalyse*, Univ. Hamburg.
[115] Roos E (1998) *Anwendungsorientierte Meß- und Berechnungsverfahren zur Kalibrierung offline programmierter Roboterapplikationen. Diss.*Hamburg .
[116] Bauer J (2011) *Methoden Der Offline-Bahnkorrektur Für Die Spanende Bearbeitung Mit Industrierobotern. Dissertation*, TU Darmstadt.
[117] Ergebnisbericht zum Verbundvorhaben. Hochproduktive generative Produktherstellung durch laserbasiertes, hybrides Fertigungskonzept. PROGEN. Fraunhofer IRB Verlag. Dresden. September 2018.
[118] Rösch O. Steigerung der Arbeitsgenauigkeit bei der Fräsbearbeitung metallischer Werkstoffe mit Industrierobotern. Zugl.: München, Techn. Univ., Fak. für Maschinenwesen. Dissertation, 2014. München: Utz, 2015.
[119] Lienenlüke L, Gründel L, Storms S, Brecher C (2018) Model-Based Process Planning for Milling Operations Using Industrial Robots. *3rd International Conference on Control and Robotics Engineering*. 978-1-5386-6662-3 (to be published end of 2018).
[120] Robotic Counter Sinking Cell. https://bit.ly/2rcvCUT. Accessed 17 May 2018.
[121] Möller C, Schmidt HC, Koch P, Böhlmann C, Kothe SM, Wollnack J, Hintze W (2017) Machining of Large Scaled CFRP-Parts with Mobile CNC-Based Robotic System in Aerospace Industry. *Procedia Manufacturing* 14:17–29.
[122] Cognitively enhanced robot for flexible manufacturing of metal and composite parts (COROMA). https://www.coroma-project.eu/. Accessed 23 March 2018.
[123] Susemihl H, Moeller C, Kothe S, Schmidt H, et al (2016) High Accuracy Mobile Robotic System for Machining of Large Aircraft Components. *SAE International Journal of Aerospace* 9(2):231–238. http://dx.doi.org/10.4271/2016-01-2139.
[124] Leali F, Pellicciari M, Pini F, Berselli G, Vergnano A (2013) An Offline Programming Method for the Robotic Deburring of Aerospace Components. Neto P, Moreira AP, (Eds.) *Robotics in Smart Manufacturing Communications in Computer a Information Science*, vol. 371. Springer, Berlin Heidelberg.
[125] Mohammad M, Babriya V, Sobh T (2008) Modeling a Deburring Process, Using DELMIA V5. *Journal of Engineering and Applied Sciences* 3(11):835–847.
[126] Princely L, Selvaraj T (2014) Vision Assisted Robotic Deburring of Edge Burrs in Cast Parts. *Procedia Engineering* 97:1906–1914.
[127] Chung J (2007) Modeling and Control of a New Robotic Deburring System. *Journal of Manufacturing Science and Engineering* 129(5):965–972.
[128] Jayaweera N, Webb P (2011) Robotic Edge Profiling of Complex Components. *Industrial Robot an International Journal* 38:38–47.
[129] Zhang H, Chen H, Xi N, Zhang G, He J (2006) On-Line Path Generation for Robotic Deburring of Cast Aluminium Wheels. *IEEE Conf on Intel Rob and Syst 2006*.
[130] Song H, Song J (2013) Precision Robotic Deburring Based on Force Control for Arbitrarily Shaped Workpiece Using CAD Model Matching. *International Journal of Precision Engineering and Manufacturing* 14(1):85–91.
[131] Villagrossi E, Pedrocchi N, Beschi M, Tosatti LM (2018) A Human Mimicking Control Strategy For Robotic Deburring of Hard Materials. *International Journal of Computer Integrated Manufacturing*.
[132] Dietz T, Schneider U, Barho M, Oberer-Treitz S, Drust M, Hollmann R, Hägele M (2012) Programming System for Efficient Use of Industrial Robots for Deburring in SME Environments. *7th German Conference on Robotics. ROBOTIK*, .
[133] Kuss A, Drust M, Verl A (2016) Detection of Workpiece Shape Deviations for Tool Path Adaptation in Robotic Deburring Systems. *49th CIRP Conference on Manufacturing Systems*, .
[134] Diaz Posada JR, Kumar S, Kuss A, Schneider U, Drust M, Dietz T, Verl A (2016) Automatic Programming and Control for Robotic Deburring. *47th International Symposium on Robotics ISR 2016*, .
[135] Breun F, Wohnig W, Siegert K (1990) Werkzeugbau für prototypen, Klein- und mittelserien. *Neuere Entwicklungen in der Blechumformung* 227–243.
[136] SCHULER GmbH (1998) *Metal Forming Handbook*, Springer, Berlin, Heidelberg.
[137] Allwood JM, King GPF, Duflou J (2005) A Structured Search for Applications of the Incremental Sheet-Forming Process by Product Segmentation. *Journal of Engineering Manufacture* 219(2):239–244.
[138] Amino H, Lu Y, Maki T, Osawa S, Fukuda K, Dieless NC, (Ed.) (2002), *Forming, Prototype of Automotive Service Parts.*
[139] Bramley AN, Vollersten F, Kleiner M (2001) Incremental Sheet Forming Process for Small Batch and Prototype Parts. *Idee-Vision-Innovation Verlag Meisenbach Bamberg* 95–102.
[140] Jeswiet J (2005) Asymmetric Incremental Sheet Forming. Advanced Materials Research. *Proceedings of the 11th International Conference on Sheet Metal — SheMet* 6-8:35–58.
[141] Meier H, Buff B, Laurischkat R, Smukala V (2009) Increasing the Part Accuracy in Dieless Robot-Based Incremental Sheet Metal Forming. *CIRP Annals Manufacturing Technology* 58:233–238.
[142] Smukala V (2012) Systematische untersuchung der druckspannungs-überlagerung in der roboterbasierten inkrementellen blechumformung, dissertation, Ruhr-Universität Bochum. *Lehrstuhl für Produktionssysteme*.
[143] Buff B, Magnus C, Zhu J, Meier H (2013) Robot-Based Incremental Sheet Metal Forming — Increasing the Geometrical Complexity and Accuracy. Key Engineering Materials. *Proceedings of the 15th International Conference on Sheet Metal — SHEMET 2013* 549:149–155.
[144] Störkle DD, Möllensiep D, Thyssen L, Kuhlenkötter B (2018) Geometry-Dependent Parameterization of Local Support in Robot-Based Incremental Sheet Forming. *Procedia Manufacturing* 15:1164–1169.
[145] Meier H, Zhu J, Buff B, Laurischkat R (2012) CAx Process Chain for Two Robots Based Incremental Sheet Metal Forming. *Procedia CIRP* 3:37–42.
[146] Laurischkat R (2012) *Kompensation prozesskraftbedingter Bahnfehler bei der roboterbasierten inkrementellen Blechumformung, Dissertation*, Ruhr-Universität Bochum, Lehrstuhl für Produktionssysteme.
[147] Li Y, Liu Z, Lu H, Daniel WJT, Liu S, Meehan PA (2014) Efficient Force Prediction for Incremental Sheet Forming and Experimental Validation. *The International Journal of Advanced Manufacturing Technology* 73(1-4):571–587.
[148] Wang J, Nair M, Zhang Y (2017) An Efficient Force Prediction Strategy for Single Point Incremental Sheet Forming. *The International Journal of Advanced Manufacturing Technology* 92(9-12):3931–3939.
[149] Abele E, Bauer J, Hemker T, Laurischkat R, Meier H, Reese S, von Stryk O (2011) Comparison and Validation of Implementations of a Flexible Joint Multibody Dynamics System Model for an Industrial Robot. *CIRP Journal of Manufacturing Science and Technology* 4(1):38–43.
[150] Hands Off Dies and Molds. *The Open Industrial & Manufacturing Engineering Journal* 14(October).
[151] Bogue R (2009) Finishing Robots: A Review of Technologies and Applications. *Industrial Robot an International Journal* 36(1):6–12.
[152] Takeuchi Y, Asakawa N, Ge D (1993) Automation of Polishing Work By an Industrial Robot: System of Polishing Robot. *JSME International Journal Series C Dynamics Control Robotics Design and Manufacturing* 36(4):556–561.
[153] Mizugaki Y, Sakamoto M, Kamijo K, Taniguchi N (1990) Development of Metal-Mold Polishing Robot System With Contact Pressure Control Using CAD/CAM Data. *CIRP Annals-Manufacturing Technology* 39(1):523–526.
[154] Saito K, Miyoshi T, Sasaki T (1993) Automation of Polishing Process for a Cavity Surface on Dies and Molds by Using an Expert System. *CIRP Annals-Manufacturing Technology* 42(1):553–556.
[155] Mizugaki Y, Sakamoto M, Sata T (1992) Fractal Path Generation for a Metal-Mold Polishing Robot System and Its Evaluation by the Operability. *CIRP Annals Manufacturing Technology* 41(1):531–534.
[156] Tam HY, Lui OCH, Mok AC (1999) Robotic Polishing of Free-Form Surfaces Using Scanning Paths. *Journal of Materials Processing Technology* 95(1-3):191–200.
[157] Márquez JJ, Pérez JM, R??ios J, Vizán A (2005) Process Modeling for Robotic Polishing. *Journal of Materials Processing Technology* 159(1):69–82.
[158] Tsai MJ, Fang JJ, Chang JL (2004) Robotic Path Planning for an Automatic Mold Polishing System. *International Journal of Robotics and Automation* 19 (2):81–90.
[159] Tsai MJ, Huang JF, Kao WL (2009) Robotic Polishing of Precision Molds with Uniform Material Removal Control. *International Journal of Machine Tools and Manufacture* 49(11):885–895.
[160] Yang Z, Xi F, Wu B (2005) A Shape Adaptive Motion Control System with Application to Robotic Polishing. *Robotics and Computer-integrated Manufacturing* 21(4-5):355–367.
[161] Sabourin M, Paquet F, Hazel B, Côté J, Mongenot P (2010) Robotic Approach to Improve Turbine Surface Finish. *Applied Robotics for the Power Industry (CARPI) 2010 1st International Conference* 1–6.
[162] Ryuh BS, Park SM, Pennock GR (2006) An Automatic Tool Changer and Integrated Software for a Robotic Die Polishing Station. *Mechanism and Machine Theory* 41(4):415–432.
[163] Tian F, Lv C, Li Z, Liu G (2016) Modeling and Control of Robotic Automatic Polishing For Curved Surfaces. *CIRP Journal of Manufacturing Science and Technology* 14:55–64.
[164] Denkena B, Lepper T (2015) Enabling an Industrial Robot for Metal Cutting Operations. *Procedia CIRP* 35:79–84.
[165] Denkena B, Brüning J, Windel L, Euhus D, Kirsch S, Overbeck D, Lepper T (2017) Holistic Process Planning Chain For Robot Machining. *Production Engineering* 111(9):515.
[166] Iglesias I, Sebastián MA, Ares JE (2015) Overview of the State of Robotic Machining: Current Situation and Future Potential. *Procedia Engineering* 132:911–917.
[167] Puzik A, Meyer C, Verl A (2010) Robot Machining With Additional 3D-Piezo-Actuation Mechanism for Error Compensation. *41st International Symposium on Robotics (ISR) & 6th German Conference on Robotics (ROBOTIK)* 415–421.
[168] Furtado LFF, Villani E, Trabasso LG, Sutério R (2017) A Method to Improve the Use of 6-dof Robots as Machine Tools. *The International Journal of Advanced Manufacturing Technology* 92:2487–2502.
[169] Abele E, Weigold M, Kulok M (2005) *Spanende Bearbeitung mit Industrierobotern: Statische und dynamische Analyse der vollseriellen Kinematik*95 .
[170] Abele E, Weigold M (2007) *Steigerung der Genauigkeit und Bauteilqualität bei der spanenden Bearbeitung mit Industrierobotern*.
[171] Kurze M (2008) *Modellbasierte Regelung von Robotern mit elastischen Gelenken ohne abtriebsseitige Sensorik*München .
[172] Weigold M (2008) *Kompensation der Werkzeugabdrängung bei der spanenden Bearbeitung mit Industrierobotern*Shaker, Darmstadt .
[173] Karim A, Waibel A, Lechler A (2016) *Experimentelle Posenanalyse am Bearbeitungsroboter: Ermittlung der Richtungs- sowie Posenabhängigkeit von Industrierobotern für die Fräsbearbeitung 106*p. 347 .
[174] Brecher C, Lienenlüke L, Obdenbusch M (2017) *Spanende Bearbeitung mit Industrierobotern: Modellbasierte Planungsassistenz für die roboterbasierte Bearbeitung 107*346–351.
[175] Abele E, Bauer J, Stelzer M, von Stryk O (2008) *Wechselwirkung von Fräsprozess und Maschinenstruktur am Beispiel des Industrieroboters*733–737.

[176] Ozturk E, Barrios A, Sun C, Rajabi S, Munoa J (2018) Robotic Assisted Milling for Increased Productivity. *CIRP Annals Manufacturing Technology*. http://dx.doi.org/10.1016/j.cirp.2018.04.031.
[177] Denkena B, Bergmann B, Lepper T (2017) Design and Optimization of a Machining Robot. *Procedia Manufacturing* 14:89–96.
[178] Denkena B, Immel J, Schönherr M (2011) Adaptronic Systems in Robot Manufacturing. *Advanced Materials Research* ;(383-390)1013–1018.
[179] Denkena B, Litwinski K, Schönherr M (2013) Innovative Drive Concept for Machining Robots. *Procedia CIRP* 9:67–72.
[180] Baier C (2017) Process and Software Chain for Combined Laser Cladding and Milling in Robot Systems. *9th International Laser Symposium*.
[181] Abele (2017) Besser qualitätsschleifen. *Form Werkzeug Carl Hanser Verlag München* 26(4):62–63. ISSN 1439-667X.
[182] König M (2016) *Sinumerik-gesteuerte Montage und Zerspanung von Motoren bei Siemens, Technologietag "Zerspanen mit Industrierobotern"*. Darmstadt.
[183] Kohkonen KE, Potdar N (1998) Composite Machining. in Peters ST, (Ed.) *Handbook of Composites*., Springer, Boston, MA.
[184] Yim M, et al (2007) Modular Self-Reconfigurable Robot Systems [Grand Challenges of Robotics]. *IEEE Robotics & Automation Magazine* 14(1):43–52.
[185] Fukuda T, Nakagawa S, Kawauchi Y, Buss M (1989) Structure Decision Method for Self Organising Robots Based on Cell Structures-CEBOT. *Proceedings of the 1989 International Conference on Robotics and Automation*, 695–700.
[186] Yim M (1994) New Locomotion Gaits. *Proceedings of the 1994 IEEE International Conference on Robotics and Automation*, 2508–2514.
[187] Murata S, Yoshida E, Kamimura A, Kurokawa H, Tomita K, Kokaji S (2002) M-TRAN: Self-Reconfigurable Modular Robotic System. *IEEE/ASME Transactions on Mechatronics: A Joint Publication of the IEEE Industrial Electronics Society and the ASME Dynamic Systems and Control Division* 7(4):431–441.
[188] Castano A, Behar A, Will PM (2002) The Conro Modules for Reconfigurable Robots. *IEEE/ASME Transactions on Mechatronics: A Joint Publication of the IEEE Industrial Electronics Society and the ASME Dynamic Systems and Control Division* 7(4):403–409.
[189] Jørgensen MW, Østergaard EH, Lund HH (2004) Modular ATRON: Modules for a Self-Reconfigurable Robot. *Proceedings of 2004 IEEE/RSJ International Conference on Intelligent Robots and Systems*, .
[190] Lyder A, Garcia RFM, Stoy K (2008) Mechanical Design of Odin, an Extendable Heterogeneous Deformable Modular Robot. *2008 IEEE/RSJ International Conference on Intelligent Robots and Systems* 883–888.
[191] Sproewitz A, Billard A, Dillenbourg P, Ijspeert AJ (2009) Roombots-Mechanical Design Of Self-Reconfiguring Modular Robots for Adaptive Furniture. *2009 IEEE International Conference on Robotics and Automation* ;(c)4259–4264.
[192] Davey J, Kwok N, Yim M (2012) Emulating Self-Reconfigurable Robots - Design of the SMORES System. *IEEE International Conference on Intelligent Robots and Systems*, 4464–4469.
[193] Gilpin K, Kotay K, Rus D, Vasilescu I (2008) Miche: Modular Shape Formation By Self-Disassembly. *The International Journal of Robotics Research* 27(3–4):345–372.
[194] Yim M, Duff D, Roufas K (2000) Polybot: a Modular Reconfigurable Robot. *IEEE International Conference on Robotics and Automation*, 514–520.
[195] Liedke J, Wörn H (2011) CoBoLD — A Bonding Mechanism For Modular Self-Reconfigurable Mobile Robots. *2011 IEEE International Conference on Robotics and Biomimetics ROBIO 2011* 2025–2030.
[196] Thorne CE, Skorodinski N, Tipton H, Van Schoyck T, Yim M (2010) Brake Design for Dynamic Modular Robots. *Proceedings — IEEE International Conference on Robotics and Automation*, 3135–3140.
[197] Vespignani M, Senft E, Bonardi S, Moeckel R, Ijspeert AJ (2013) An Experimental Study on the Role of Compliant Elements on the Locomotion of the Self-Reconfigurable Modular Robots Roombots. *IEEE International Conference on Intelligent Robots and Systems*, 4308–4313.
[198] Catalano MG, et al (2011) VSA-CubeBot: A Modular variable Stiffness Platform for Multiple Degrees of Freedom Robots. *Proceedings — IEEE International Conference on Robotics and Automation*, 5090–5095.
[199] Aghili F, Parsa K (2009) A Reconfigurable Robot with Lockable Cylindrical Joints. *IEEE Transactions on Robotics: A Publication of the IEEE Robotics and Automation Society* 25(4):785–797.
[200] Pan X, Wang H, Jiang Y, Yu C (2011) Research on Kinematics of Modular Reconfigurable Robots. *2011 IEEE International Conference on Cyber Technology in Automation, Control, and Intelligent Systems, CYBER 2011*, 91–96.
[201] Huang T, Li M, Zhao XM, Mei JP, Chetwynd DG, Hu SJ (2005) Conceptual Design And Dimensional Synthesis for a 3-DOF Module of the TriVariant — A Novel 5-DOF Reconfigurable Hybrid Robot. *IEEE Transactions on Robotics: A Publication of the IEEE Robotics and Automation Society* 21(3):449–456.
[202] Wu W, et al (2013) Task-Oriented Inverse Kinematics of Modular Reconfigurable Robots. *2013 IEEE/ASME International Conference on Advanced Intelligent Mechatronics: Mechatronics for Human Wellbeing* 1187–1192.
[203] Köker R (2013) A Genetic Algorithm Approach to a Neural-Network-Based Inverse Kinematics Solution of Robotic Manipulators Based on Error Minimization. *Information Sciences* 222:528–543.
[204] Qiao G, Song G, Zhang J, Sun H, Ge J, Wang W (2012) Design of a Self-Reconfigurable Wireless Network System for Modular Self-Reconfigurable Robots. *2012 IEEE International Conference on Robotics and Biomimetics, ROBIO 2012 — Conference Digest*, 1337–1342.
[205] Bordignon M, Stoy K, Schultz UP (2011) Generalized Programming of Modular Robots Through Kinematic Configurations. *IEEE International Conference on Intelligent Robots and Systems*, 3659–3666.
[206] Castro S, Koehler S, Kress-Gazit H (2011) High-Level Control of Modular Robots. *International Conference on Intelligent Robots and Systems*, 3120–3125.
[207] Hofbaur M, Brandstötter M, Jantscher S, Schörghuber C (2010) Modular Re-Configurable Robot Drives. *2010 IEEE Conference on Robotics, Automation and Mechatronics, RAM 2010*, 150–155.
[208] Vonasek V, Saska M, Kosnar K, Preucil L (2013) Global Motion Planning for Modular Robots With Local Motion Primitives. *Proceedings - IEEE International Conference on Robotics and Automation*, 2465–2470.
[209] Hou F, Shen WM (2010) On the Complexity of Optimal Reconfiguration Planning for Modular Reconfigurable Robots. *Proceedings - IEEE International Conference on Robotics and Automation*, 2791–2796.
[210] Lin Y, Xi F, Mohamed RP, Tu X-W (2010) Calibration of Modular Reconfigurable Robots Based on a Hybrid Search Method. *Journal of Manufacturing Science and Engineering ASME* 132(no. 6):610021–610028.
[211] Mohamed RP, Xi Jr F, Finistauri AD (2010) Module-Based Static Structural Design of a Modular Reconfigurable Robot. *Journal of Mechanical Design* 132 (1):014501.
[212] Valente A (2016) Reconfigurable Industrial Robots: A Stochastic Programming Approach For Designing and Assembling Robotic Arms. *Robotics and Computer-integrated Manufacturing* 41:115–126.
[213] Galar Pascual D (2015) *Artificial Intelligence Tools — Decision Support Systems in Condition Monitoring and Diagnosis*, CRC Press.
[214] Jaber AA, Bicker R (2014) The State Of The Art In Research Into The Condition Monitoring Of Industrial Machinery. *International Journal of Current Engineering and Technology* 4(3):1986–2001.
[215] Elosegui P (1992) Measurement of the Dynamic Model of a Puma 560 Robot Using Experimental Modal Analysis. *Journal of Mechanical Design* 116 (1):75–79.
[216] Pan MC, Van Brussel H, Sas P (1998) Intelligent Joint Fault Diagnosis of Industrial Robots. *Mechanical Systems and Signal Processing* 12(4):571–588.
[217] Liu H, Wei T, Wang X (2009) Signal Decomposition and Fault Diagnosis of a Scara Robot Based Only on Tip Acceleration Measurement. *IEEE International Conference on Mechatronics and Automation ICMA*, 4811–4816.
[218] Trendafilova I, Van Brussel H (2003) Condition Monitoring of Robot Joints Using Statistical and Nonlinear Dynamics Tools. *Meccanica* 38(2):283–295.
[219] Valente A, Carpanzano E (2011) Development of Multi-Level Adaptive Control And Scheduling Solutions For Shop-Floor Automation In Reconfigurable Manufacturing Systems. *CIRP Annals — Manufacturing Technology* 60 (1):449–452.
[220] Deisenroth MP, Neumann G, Peters J (2011) A Survey On Policy Search For Robotics. *Foundations and Trends in Robotics* 2(1–2):1–142.
[221] Levine S, Finn C, Darrell T, Abbeel P (2016) "End-to-End Training of Deep Visuomotor Policies. *Journal of Machine Learning Research* 17(1):1334–1373.
[222] Chebotar Y, Kalakrishnan M, Yahya A, Li A, Schaal S, Levine S (2017) Path Integral Guided Policy Search. *Proceedings — IEEE International Conference on Robotics and Automation*, 3381–3388.
[223] Peters J, Schaal S (2008) Reinforcement Learning of Motor Skills With Policy Gradients. *Neural Networks* 21(4):682–697.
[224] Riedmiller M (2005) Neural Fitted Q Iteration — First Experiences With a Data Efficient Neural Reinforcement Learning Method. *Lecture Notes in Computer Science (including subseries Lecture Notes in Artificial Intelligence and Lecture Notes in Bioinformatics)* 3720:317–328. LNAI.
[225] Mnih V, et al (2016) Asynchronous Methods for Deep Reinforcement Learning. *International Conference on Machine Learning*, 1928–1937.
[226] Nikolaidis S, Lasota P, Rossano G, Martinez C, Fuhlbrigge T, Shah J (2013) Human-Robot Collaboration in Manufacturing: Quantitative Evaluation of Predictable, Convergent Joint Action. *44th International Symposium on Robotics*.
[227] Cencen A, Verlinden JC, Geraedts J (2016) Qualifying the Performance of Human Robot Coproduction at a Relabling Station. *TMCE 2016*.
[228] Chhim P, Chinnam RB, Sadawi N (2017) Product Design and Manufacturing Process Based Ontology For Manufacturing Knowledge Reuse. *Journal of Intelligent Manufacturing* 1–12.
[229] Zhang Y, Huang GQ, Sun S, Yang T (2014) Multi-agent Based Real-Time Production Scheduling Method For Radio Frequency Identification Enabled Ubiquitous Shopfloor Environment. *Computers & Industrial Engineering* 76 (1):89–97.
[230] Wu D, Rosen DW, Wang L, Schaefer D (2015) Cloud-Based Design and Manufacturing: A New Paradigm in Digital Manufacturing and Design Innovation. *Computer-Aided Design* 59:1–14.